

RESEARCH ARTICLE

10.1002/2016JC011816

Carbon export fluxes and export efficiency in the central Arctic during the record sea-ice minimum in 2012: a joint $^{234}\text{Th}/^{238}\text{U}$ and $^{210}\text{Po}/^{210}\text{Pb}$ studyMontserrat Roca-Martí¹, Viena Puigcorbé^{1,2}, Michiel M. Rutgers van der Loeff³, Christian Katlein³, Mar Fernández-Méndez^{3,4}, Ilka Peeken^{3,5}, and Pere Masqué^{1,2,6}

Key Points:

- First use of $^{234}\text{Th}/^{238}\text{U}$ together with $^{210}\text{Po}/^{210}\text{Pb}$ as proxies for particulate organic carbon export in the Arctic
- Low particulate organic carbon fluxes escaping from the euphotic zone during the record sea-ice minimum in 2012
- High export efficiency of the biological pump in the central Arctic

Correspondence to:

M. Roca-Martí,
Montserrat.Roca.Marti@uab.cat
P. Masqué,
pere.masque@uab.cat

Citation:

Roca-Martí, M., V. Puigcorbé, M. M. Rutgers van der Loeff, C. Katlein, M. Fernández-Méndez, I. Peeken, and P. Masqué (2016), Carbon export fluxes and export efficiency in the central Arctic during the record sea-ice minimum in 2012: a joint $^{234}\text{Th}/^{238}\text{U}$ and $^{210}\text{Po}/^{210}\text{Pb}$ study, *J. Geophys. Res. Oceans*, 121, doi:10.1002/2016JC011816.

Received 21 MAR 2016

Accepted 14 JUN 2016

Accepted article online 16 JUN 2016

¹Institut de Ciència i Tecnologia Ambientals and Departament de Física, Universitat Autònoma de Barcelona, Barcelona, Spain, ²School of Science and Centre for Marine Ecosystems Research, Edith Cowan University, Joondalup, Western Australia, Australia, ³Alfred Wegener Institute for Polar and Marine Research, Bremerhaven, Germany, ⁴Norwegian Polar Institute, Fram Centre, Tromsø, Norway, ⁵MARUM – Center for Marine Environmental Sciences, University of Bremen, Bremen, Germany, ⁶Oceans Institute and School of Physics, University of Western Australia, Crawley, Western Australia, Australia

Abstract The Arctic sea-ice extent reached a record minimum in September 2012. Sea-ice decline increases the absorption of solar energy in the Arctic Ocean, affecting primary production and the plankton community. How this will modulate the sinking of particulate organic carbon (POC) from the ocean surface remains a key question. We use the $^{234}\text{Th}/^{238}\text{U}$ and $^{210}\text{Po}/^{210}\text{Pb}$ radionuclide pairs to estimate the magnitude of the POC export fluxes in the upper ocean of the central Arctic in summer 2012, covering time scales from weeks to months. The $^{234}\text{Th}/^{238}\text{U}$ proxy reveals that POC fluxes at the base of the euphotic zone were very low ($2 \pm 2 \text{ mmol C m}^{-2} \text{ d}^{-1}$) in late summer. Relationships obtained between the ^{234}Th export fluxes and the phytoplankton community suggest that prasinophytes contributed significantly to the downward fluxes, likely via incorporation into sea-ice algal aggregates and zooplankton-derived material. The magnitude of the depletion of ^{210}Po in the upper water column over the entire study area indicates that particle export fluxes were higher before July/August than later in the season. ^{210}Po fluxes and ^{210}Po -derived POC fluxes correlated positively with sea-ice concentration, showing that particle sinking was greater under heavy sea-ice conditions than under partially ice-covered regions. Although the POC fluxes were low, a large fraction of primary production (>30%) was exported at the base of the euphotic zone in most of the study area during summer 2012, indicating a high export efficiency of the biological pump in the central Arctic.

1. Introduction

Climate change is triggering an unprecedented decline in Arctic sea ice. In September 2012 the sea-ice cover amounted to less than half of its 1979–2000 baseline [Overland and Wang, 2013]. Such a decrease in ice extent and thickness [Haas et al., 2008] allows more sunlight to be transmitted through the sea ice, increasing the absorption of solar energy in the Arctic Ocean [Nicolaus et al., 2012] and affecting sea-ice and upper ocean ecosystems [Wassmann, 2011]. Net primary production (NPP) increased by 30% between 1998 and 2012 according to a satellite-based study [Arrigo and van Dijken, 2015]. Yet this kind of approach does not take into account the productivity of either under-ice phytoplankton or sea-ice algae, even though it can be substantial [Gosselin et al., 1997; Fortier et al., 2002; Lee et al., 2010; Arrigo et al., 2012; Fernández-Méndez et al., 2015]. However, light-driven increments in NPP will be constrained if nutrient supply to surface waters does not increase considerably by mixing or upwelling [e.g., Tremblay et al., 2015]. Besides this, enhanced NPP does not necessarily mean larger export fluxes of particulate organic carbon (POC) to the deep ocean, since the changing Arctic scenario favors a phytoplankton community structure based on the smallest cells [Li et al., 2009]. Overall, it remains uncertain how the changes in NPP and plankton community will affect the sinking of POC from the ocean surface, and in turn contribute to the marine sequestration of CO_2 [Honjo et al., 2010; Anderson and Macdonald, 2015].

To date, the Arctic Ocean is considered a weak sink for atmospheric CO_2 , accounting for ~6% of the global oceanic uptake [Gruber et al., 2009]. An essential component of the ocean carbon sink is the “biological pump” driven by the export of organic particles from the ocean surface to its interior [Falkowski et al., 1998]. During the

productive season, the surface downward fluxes of POC are widely heterogeneous in the Arctic, reaching higher values ($>30 \text{ mmol C m}^{-2} \text{ d}^{-1}$) over the shelves [e.g., Cochran *et al.*, 1995b; Lepore *et al.*, 2007] in comparison to the central Arctic ($<5 \text{ mmol C m}^{-2} \text{ d}^{-1}$) [e.g., Moran *et al.*, 1997; Cai *et al.*, 2010]. However, in summer 2012, a widespread deposition of ice algal biomass on the seafloor ($>3000 \text{ m}$, median estimate of $750 \text{ mmol C m}^{-2}$) was observed in the central Arctic associated with rapid ice melt [Boetius *et al.*, 2013].

The export efficiency is defined as the ratio between export and production, which indicates the strength of the biological pump [Buesseler and Boyd, 2009]. A recent model study reports a high annual mean export efficiency of $>30\%$ in Arctic waters [Henson *et al.*, 2015]. Nevertheless, primary production and export data are very scarce, especially in the interior basins [Gustafsson and Andersson, 2012; Matrai *et al.*, 2013]. Indeed, the temporal mismatch between the measurement of production and export, combined with the existence of a long lag period between both processes in the Arctic (30–40 days), makes the assessment of the export efficiency on a seasonal scale difficult [Henson *et al.*, 2015].

The radionuclide pairs $^{234}\text{Th}/^{238}\text{U}$ and, to a lesser extent, $^{210}\text{Po}/^{210}\text{Pb}$ have been used as proxies for POC export since the 1990s [Buesseler *et al.*, 1992; Shimmield *et al.*, 1995], but very few studies have used both pairs together [Verdeny *et al.*, 2009; Stewart *et al.*, 2011; Wei *et al.*, 2011; Le Moigne *et al.*, 2013a]. Several authors have recommended the simultaneous use of $^{234}\text{Th}/^{238}\text{U}$ and $^{210}\text{Po}/^{210}\text{Pb}$ since they cover different time scales, from weeks to months, respectively, and ^{234}Th and ^{210}Po have different biogeochemical behaviors, providing complementary information on POC export fluxes [Friedrich and Rutgers van der Loeff, 2002; Verdeny *et al.*, 2009; Stewart *et al.*, 2011].

In this study, we aim to estimate the magnitude of the POC fluxes at the bottom of the euphotic zone and within the upper mesopelagic layer in the central Arctic during the record sea-ice minimum in 2012, as well as identify mechanisms that control particle export by means of $^{234}\text{Th}/^{238}\text{U}$ and $^{210}\text{Po}/^{210}\text{Pb}$. The use of both pairs may shed light on the apparent mismatch between the low ^{234}Th -based export production estimates [Cai *et al.*, 2010] and the benthic observations of massive sea-ice algae deposits [Boetius *et al.*, 2013] in the central Arctic. It might also give a hint of the trend that POC fluxes may follow as the sea ice continues to decline. To this purpose we:

1. Quantify the POC export fluxes at the bottom of the euphotic zone, 50, 100, and 150 m on short-term and seasonal scales by using the $^{234}\text{Th}/^{238}\text{U}$ and $^{210}\text{Po}/^{210}\text{Pb}$ pairs.
2. Identify potential relationships between sea-ice conditions, phytoplankton community, and particle export.
3. Assess the export efficiency combining the export estimates at the bottom of the euphotic zone with daily, weekly, and annual NPP estimates.

2. Materials and Methods

2.1. Study Area

The sampling was performed from 11 August to 28 September 2012 during the ARK-XXVII/3 expedition in the Eurasian Basin of the central Arctic (2 August to 8 October 2012; R/V Polarstern [Boetius, 2013]). The survey coincided with a new record low of sea-ice cover since the beginning of satellite imagery in 1978 [Parkinson and Comiso, 2013]. The specific locations and dates of the sea-ice stations are given in Figure 1 and Table 1.

2.2. Total $^{234}\text{Th}/^{238}\text{U}$ and $^{210}\text{Po}/^{210}\text{Pb}$

Total ^{234}Th , ^{210}Po , and ^{210}Pb activities were determined from seawater samples collected using Niskin bottles attached to a CTD rosette. Twelve depth vertical profiles from 10 to 400 m were taken, with higher resolution in the upper 150 m of the water column.

Total ^{234}Th activities were determined from 4 L of seawater at nine stations. Additionally, replicates of deep samples (1500–3000 m) were collected for calibration purposes [Rutgers van der Loeff *et al.*, 2006]. The samples were processed following the MnO_2 co-precipitation technique [Buesseler *et al.*, 2001] using ^{230}Th as a chemical yield tracer [Pike *et al.*, 2005]. Briefly, the precipitates were filtered through QMA quartz fiber filters, dried overnight at 50°C , and prepared for beta counting. The counting was done on board using low background beta counters (Risø National Laboratories, Denmark). Samples were remeasured after 7 months to quantify background activities. ^{230}Th recoveries were determined in all filters by inductively coupled plasma

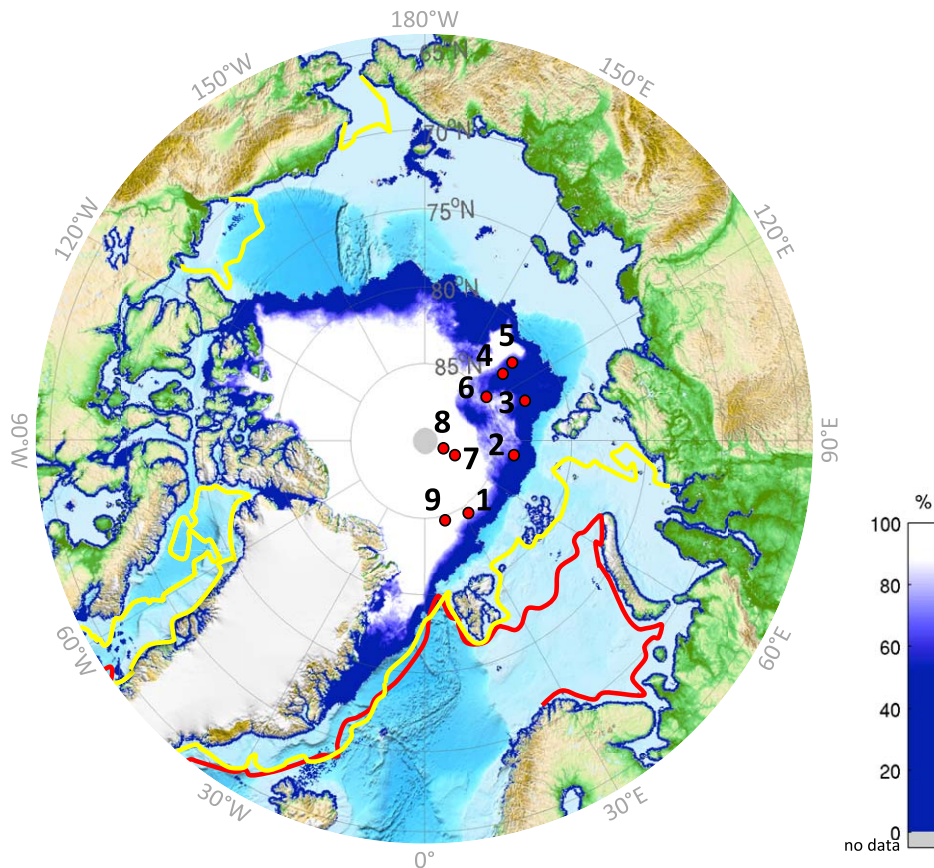


Figure 1. Location of sea-ice stations sampled during the IceArc cruise (ARK-XXVII/3, August–September 2012) (red dots). Average sea-ice concentration in September 2012. Contour lines represent the sea-ice extent in February (red) and July (yellow) 2012. Sea-ice concentration data were obtained from <http://www.meereisportal.de> [Spren et al., 2008].

mass spectrometry (ICP-MS) as described in *Roca-Martí et al.* [2016]. The average chemical recovery was $94 \pm 4\%$ ($n = 107$). The parent ^{238}U activity was derived from salinity using the relationship given by *Owens et al.* [2011]. Stations 4–6 had salinities of 30.0–32.5 from 10 to 30 m ($n = 15$), falling below the range used by *Owens et al.* [2011]. For these samples, we also applied the U-salinity relationship given by *Not et al.* [2012] determined from sea ice, surface seawater, and sea-ice brine samples, covering a wide salinity range (0–135). A difference of only 1.1% in ^{238}U activity, which is lower than its associated uncertainty (1.9–2.3%), was obtained using the two relationships, validating the use of Owens's relationship in the present study. The ^{234}Th activity uncertainties were always $\leq 6\%$, which include those uncertainties associated with counting, detector background and calibration, and ICP-MS measurements.

Total ^{210}Po and ^{210}Pb activities were determined from 11 L of seawater at seven stations using the cobalt-ammonium pyrrolidine dithiocarbamate (Co-APDC) coprecipitation technique [Fler and Bacon, 1984]. Samples were immediately acidified after collection with HCl to pH < 2 and spiked with stable Pb and ^{209}Po as chemical yield tracers. Cobalt nitrate and APDC solutions were added after at least 1 day of isotope equilibration. Samples were filtered through 0.2 μm membrane filters and stored for later processing at the home laboratory. The filters were digested using concentrated HNO_3 and samples were reconstructed with 1 M HCl. ^{210}Po and ^{210}Pb were separated by auto-deposition of polonium onto silver discs during 6 h [Flynn, 1968]. The silver discs were then counted by alpha spectrometry using passivated implanted planar silicon (PIPS) alpha detectors (Canberra, USA) and silicon surface barrier (SSB) alpha detectors (EG&G Ortec, USA). Solutions were replated and passed through an anion exchange resin (AG 1-X8) to ensure the complete elimination of polonium from samples [Rigaud et al., 2013]. Samples were respiked with ^{209}Po and stored for 9–11 months for later determination of ^{210}Pb via ^{210}Po ingrowth. At that time, samples were plated and counted once more by alpha spectrometry. ^{210}Pb and

Table 1. Location and Date of the Stations Sampled During the ARK-XXVII/3 Cruise Together With Information on Oceanographic and Sea-Ice Conditions, Chl-a Inventory at 30 m Depth, Phytoplankton Classifications by Size and Group, and NPP Estimates (See Text for Further Details)^a

Station	1	2	3	4	5	6	7	8	9
Polarstern station #	PS80/224	PS80/237	PS80/255	PS80/277	PS80/323	PS80/335	PS80/349	PS80/360	PS80/384
Longitude (°E)	31.19	75.99	110.11	129.83	131.12	123.47	60.97	57.07	17.59
Latitude (°N)	84.03	83.92	83.08	82.89	81.93	85.17	87.93	88.80	84.37
Date (2012)	9–11 Aug.	14–16 Aug.	20–22 Aug.	25–26 Aug.	4–5 Sept.	7–9 Sept.	18–19 Sept.	22–23 Sept.	28–29 Sept.
Euphotic zone depth (m) ^b	24	29	30	29	33	29	15	7	27
Mixed layer depth (m)	16	20	18	22	20	25	29	30	22
Sea-ice thickness (m) ^{b,c}	1.0	1.3	0.9	0.9	0.8	0.7	1.6	1.8	1.2
Sea-ice concentration (%) ^{b,c}	80	80	70	80	60	50	100	100	100
Chl-a inventory (mg m ⁻²)	4.8	22.8	8.9	7.0	8.9	11.2	6.1	3.3	2.5
<i>Phytoplankton Size (% Chl-a Biomass)</i>									
Microplankton	36	29	38	54	36	14	34	nd ^d	39
Nanoplankton	22	0	2	13	4	28	44	nd	32
Picoplankton	42	71	60	33	60	58	22	nd	29
<i>Phytoplankton Group (% Chl-a Biomass)</i>									
Diatoms	19	5	4	44	27	3	23	nd	22
Dinoflagellates_1	0	0	8	2	0	0	0	nd	0
Dinoflagellates_2	8	0	9	0	2	11	1	nd	12
Haptophytes_3	21	0	0	4	0	26	61	nd	19
Haptophytes_4	0	0	8	5	3	3	2	nd	4
Cryptophytes	0	0	1	18	10	0	0	nd	0
Prasinophytes_1	51	33	8	26	27	35	12	nd	22
Prasinophytes_2	0	61	61	0	28	0	0	nd	0
Pelagophytes	0	0	1	1	3	0	0	nd	21
Chlorophytes	0	0	0	0	0	21	1	nd	0
<i>NPP Estimates (mmol C m⁻² d⁻¹)</i>									
In situ	3.3	2.7	1.3	0.5	5.0	2.3	0.2	0.1	nd
One week	2.3	2.3	2.2	3.5	1.8	1.9	0.6	0.5	nd
Two weeks	2.4	2.5	2.2	3.3	2.2	2.3	0.8	0.6	nd
Annual	3.3	4.8	2.1	2.9	5.6	3.2	11.9	9.9	7.9

^a²³⁴Th/²³⁸U, ²¹⁰Po/²¹⁰Pb, and sediment traps [Lalande et al., 2014] were used to estimate POC export fluxes at all the stations, except at stations 5 and 9 for ²¹⁰Po/²¹⁰Pb.

^bData from Fernández-Méndez et al. [2015].

^cData from Katlein et al. [2014].

^dnd, no available data.

²¹⁰Po activities at sampling time were calculated applying in-growth, decay, and recovery corrections following Rigaud et al. [2013]. Two aliquots from each sample were taken before the first and last platings to determine the chemical recovery of stable Pb by inductively coupled plasma optical emission spectrometry (ICP-OES). The average recovery was 87 ± 9% (n = 83). The activity uncertainties were on average 7% for ²¹⁰Pb and 16% for ²¹⁰Po, which include those uncertainties associated with counting, detector background, and ²⁰⁹Po activity. The larger uncertainties of ²¹⁰Po are due to the time elapsed between sampling and the first Po plating (>80 days). All data of total ²³⁴Th, ²³⁸U, ²¹⁰Po, and ²¹⁰Pb activities are available at <http://doi.pangaea.de/10.1594/PANGAEA.858790>.

2.3. Particulate Fraction

Large (>53 μm) particles for analyses of ²³⁴Th, ²¹⁰Po, ²¹⁰Pb, POC, and particulate organic nitrogen (PON) were collected using in situ pumps (ISP, Challenger Oceanic, UK). Four ISP were deployed at each station at 25, 50, 100, and 150 m, filtering on average 1500 L. Particles were retained using 53 μm pore size nylon mesh screens and rinsed with filtered seawater. After homogenization, the sample was subdivided into two aliquots: one was filtered through precombusted QMA filters to analyze ²³⁴Th, POC, and PON on the same filter, and the other aliquot was filtered through QMA filters to analyze ²¹⁰Po and ²¹⁰Pb. Swimmers observed by naked eye were picked from all samples. The activity of ²³⁴Th in particles

was measured by beta counting as described for the water samples. POC and PON were determined with an EuroVector Elemental Analyzer, pretreating the filters with diluted HCl [Knap *et al.*, 1996]. The results were corrected for POC and PON blanks (1.7 ± 0.1 and 0.35 ± 0.06 μmol , respectively), representing on average 5 and 8% of the POC and PON measurements, respectively. The filters for ^{210}Po and ^{210}Pb determination were spiked with ^{209}Po and stable Pb, digested using a mixture of concentrated HNO_3 , HCl, and HF, evaporated to dryness and reconstructed with 1 M HCl. Samples were processed and measured by alpha spectrometry as described for the water samples. All data of particulate ^{234}Th , ^{210}Po , ^{210}Pb , and organic carbon, and nitrogen concentrations are available at <http://doi.pangaea.de/10.1594/PANGAEA.858790>.

2.4. Pigments

One liter of seawater samples were taken from Niskin bottles attached to the CTD rosette from three to four depths in the upper 30 m at eight stations. The samples were immediately filtered on GF/F filters, frozen in liquid nitrogen, and stored at -80°C until further analyses by high-performance liquid chromatography (HPLC) at the home laboratory. The samples were measured using a Waters 600 controller equipped with an auto sampler (717 plus), a photodiode array detector (2996), a fluorescence detector (2475), and the EMPOWER software. Fifty microliter of internal standard (canthaxanthin) and 1.5 mL acetone were added to each filter vial and then homogenized for 20 s in a Precellys tissue homogenizer. After centrifugation the supernatant liquids were filtered through 0.2 μm PTFE filters (Rotilabo) and placed in Eppendorf cups. Aliquots of 100 μL were transferred to the auto-sampler (4°C), premixed with 1 M ammonium acetate solution in a 1:1 volume ratio just prior to analysis, and injected onto the HPLC-system. Pigments were analyzed by reverse-phase HPLC using a VARIAN Microsorb-MV3 C8 column (4.6×100 mm) and HPLC-grade solvents (Merck). Solvent A consisted of 70% methanol and 30% 1 M ammonium acetate, and solvent B contained 100% methanol. The gradient was modified after Barlow *et al.* [1997]. Eluted pigments were detected by absorbance (440 nm) and fluorescence (Ex: 410 nm, Em: >600 nm). Pigments were identified by comparing their retention times with those of pure standards. Additional confirmation for each pigment was done by comparing the sample spectra with online diode array absorbance spectra between 390 and 750 nm stored in the library. Pigment concentrations were quantified based on peak areas of external standards, which were spectrophotometrically calibrated using extinction coefficients published by Bidigare [1991] and Jeffrey *et al.* [1997]. The taxonomic structure of the phytoplankton groups (diatoms, dinoflagellates_1, dinoflagellates_2, haptophytes_3, haptophytes_4, cryptophytes, prasinophytes_1, prasinophytes_2, pelagophytes, and chlorophytes) was calculated from marker pigment ratios using the CHEMTAX program [Mackey *et al.*, 1996]. Pigment ratios were constrained as suggested by Higgins *et al.* [2011] based on molecular analyses of 18S rDNA [Kilias *et al.*, 2013] and microscopic examination of representative samples. Phytoplankton size classes (micro-, nano-, and picoplankton) were estimated according to Uitz *et al.* [2006] and Hirata *et al.* [2011], summarized by Taylor *et al.* [2011]. Microplankton corresponded to phytoplankton with size between 20 and 200 μm , nanoplankton between 2 and 20 μm , and picoplankton <2 μm . The phytoplankton classifications by group and size are expressed as percentage of total chlorophyll a (Chl-a) biomass.

2.5. Primary Production

In situ NPP was measured at eight stations using the ^{14}C uptake method [Steemann Nielsen, 1952], with minor modifications as described in Fernández-Méndez *et al.* [2015]. Seawater, melted sea-ice cores and melt pond samples (one 200 mL sample per environment and station) were spiked with 0.1 $\mu\text{Ci mL}^{-1}$ of ^{14}C labeled sodium bicarbonate (Moravek Biochemicals, USA) and incubated for 12 h at -1.3°C under different scalar irradiances ($0\text{--}420$ $\mu\text{mol photons m}^{-2} \text{s}^{-1}$). Depth-integrated in situ rates were calculated for each environment as a function of the available photosynthetically active radiation (PAR) using the photosynthetic parameters obtained in the photosynthesis versus irradiance curves. Water column production was integrated over the euphotic zone (1% of incoming PAR) and sea-ice algae production over the length of the ice cores retrieved.

At the same stations we calculated the integrated amount of NPP that potentially occurred 1 and 2 weeks before sampling using the Central Arctic Ocean Primary Productivity (CAOPP) model [Fernández-Méndez *et al.*, 2015]. This model calculates NPP from incident light and sea-ice conditions based on different remote-sensing data sets on the basis of photosynthesis-irradiance curves measured during the cruise. NPP was calculated for each day during the 14 days prior to sampling, summed up to integrate values for the 1

and 2 week period before sampling, and divided by 7 and 14 days, respectively, to obtain average daily rates for these two periods.

Annual new NPP was calculated from the nitrate drawdown in the mixed layer since previous winter at nine stations, as described in *Fernández-Méndez et al.* [2015]. The annual total inorganic nitrogen uptake was then transformed to carbon units using the Redfield ratio 106C:16N [*Smith et al.*, 1997; *Codispoti et al.*, 2013], giving annual new NPP estimates for sea ice and water column during the Arctic productive season. To calculate an average daily rate, we assumed a productive season of 120 days [*Gradinger et al.*, 1999]. Although most of the new NPP occurs before late summer, we note that these estimates may be underestimated, especially for the first stations sampled in August. This method assumes that lateral input of nitrate from rivers or shelves is negligible, which should be the case of the present study ($>81^{\circ}\text{N}$) due to its consumption in Arctic shelf waters [*Le Fouest et al.*, 2013]. Further, this method does not take into consideration nitrification and upward flux of nitrate, which are assumed to have a relatively small contribution to the nitrate concentrations in the mixed layer in comparison with the biological uptake.

3. Results

3.1. Study Area

Sea-ice conditions, phytoplankton communities, and primary production rates in the study area are described below and summarized in Table 1.

3.1.1. Oceanographic and Sea-Ice Conditions

Stations were located over the deep Arctic (>3000 m) in the Nansen (stations 1–3 and 9) and Amundsen Basins (stations 4–8, Figure 1). The sea-ice conditions encountered during the expedition are described in *Katlein et al.* [2014]. Stations located north of 87°N (stations 7 and 8) had multiyear ice, 1.6–1.8 m thick, while the rest consisted of degraded first-year ice of 0.7–1.3 m. The sea-ice concentration varied from 50 to 80% at stations 1–6, but it was 100% at those stations visited in mid-late September (stations 7–9, Table 1). The coverage of melt-ponds ranged from 10 to 50% [*Boetius et al.*, 2013]. The euphotic zone was on average 25 m deep and was nutrient-depleted by phytoplankton consumption: (i) silicate-depleted at stations 1–3; (ii) nitrate-depleted at stations 4 and 5; and (iii) silicate, nitrate, and phosphate-depleted at stations 6–9 [*Fernández-Méndez et al.*, 2015]. The mixed layer was on average 22 m thick and was defined by the depth where density increased from its surface value to 20% of the difference between 100 m and the surface [*Shaw et al.*, 2009] using the CTD profiles obtained during the cruise (doi:10.1594/PAN-GAEA.802904). The winter mixed layer depth was found at around 55 m [*Fernández-Méndez et al.*, 2015] above the lower halocline (salinity range: 33.5–34.5) [*Rudels*, 2009], which reached depths down to 115 m. The potential temperature maximum indicative of the Atlantic Water core was found between 180 and 290 m. The Arctic intermediate waters as well as deep and bottom waters were present below the warm Atlantic layer.

3.1.2. Biology

The Chl-*a* inventories in the upper 30 m of the water column were on average 8.4 ± 6.1 mg m^{-2} , with a maximum at station 2 (22.8 mg m^{-2}) and a minimum at station 9 (2.5 mg m^{-2}). The phytoplankton community was picoplankton dominated at many stations (1, 2, 3, 5, and 6), accounting for ~ 40 – 70% of the total Chl-*a* biomass. At those stations prasinophytes were the most relevant group with a relative biomass of up to 95%. Large cells dominated the community at station 4 with a significant contribution from diatoms (44%), while nanoplankton prevailed at station 7 with a dominance of haptophytes (63%). Finally, station 9 had a similar biomass distribution between size classes (Table 1).

The integrated in situ NPP rates in the euphotic zone, sea ice, and melt ponds ranged from 0.1 $\text{mmol C m}^{-2} \text{d}^{-1}$ at the northernmost station (8) to 5.0 $\text{mmol C m}^{-2} \text{d}^{-1}$ at the southernmost station (5). In situ NPP was highest at the picoplankton-dominated stations (>1.3 $\text{mmol C m}^{-2} \text{d}^{-1}$). The daily NPP estimates during 1 and 2 weeks prior to sampling were higher than the in situ estimates by a factor of 2–7 at stations 3, 4, 7, and 8, while they were a factor of 3 lower at station 5. These estimates were comparable at stations 1, 2, and 6. The annual new primary production estimates compared well with the in situ, 1 and 2 week daily estimates from stations 1–6. However, north of 87°N (stations 7 and 8) the annual estimates were higher than the average of the other estimates by a factor >20 (~ 10 – 12 $\text{mmol C m}^{-2} \text{d}^{-1}$, Table 1).

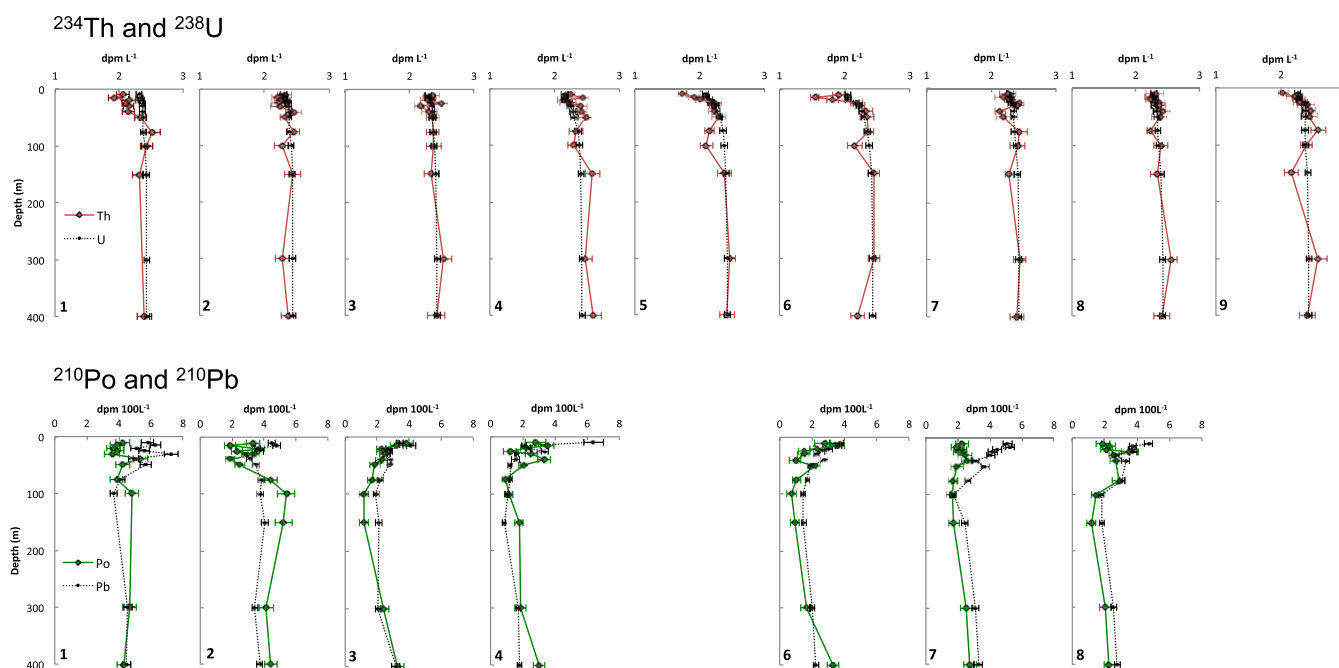


Figure 2. Vertical activity profiles for ^{234}Th (red solid line) and ^{238}U (dotted line) (top) and for ^{210}Po (green solid line) and ^{210}Pb (dotted line) (bottom), from 10 to 400 m depth. ^{238}U was derived from salinity [Owens *et al.*, 2011].

3.2. Total $^{234}\text{Th}/^{238}\text{U}$ and $^{210}\text{Po}/^{210}\text{Pb}$

3.2.1. Seawater Profiles

The profiles of the total activities of ^{234}Th and ^{238}U , and ^{210}Po and ^{210}Pb are illustrated in Figure 2.

The specific activities of each radionuclide ranged from 1.54 ± 0.06 to 2.59 ± 0.13 dpm L^{-1} for ^{234}Th , 2.04 ± 0.05 to 2.44 ± 0.05 dpm L^{-1} for ^{238}U , 0.7 ± 0.3 to 5.4 ± 0.5 dpm 100L^{-1} for ^{210}Po , and 0.84 ± 0.09 to 7.3 ± 0.4 dpm 100L^{-1} for ^{210}Pb . Within the upper 25 m of the water column, significant deficits of ^{234}Th (i.e., $^{234}\text{Th}/^{238}\text{U} < 0.9$, given uncertainties) were observed at stations 1, 5, and 6, while significant deficits of ^{210}Po (i.e., $^{210}\text{Po}/^{210}\text{Pb} < 0.8$, given uncertainties) were detected at all the stations. Below 25 m depth, deficits of ^{234}Th were detected at one single depth at stations 5 and 9 (at 100 and 150 m, respectively), but deficits of ^{210}Po were found at every station usually at several depths (30–150 m). Excesses of ^{234}Th (i.e., $^{234}\text{Th}/^{238}\text{U} > 1.1$) were not observed at any profile below 25 m, whereas excesses of ^{210}Po (i.e., $^{210}\text{Po}/^{210}\text{Pb} > 1.2$) were observed at four stations (1, 2, 4, and 6).

Station 1 showed deficits of ^{234}Th and ^{210}Po within the upper 50 m: 11500 ± 2100 and 770 ± 120 dpm m^{-2} , respectively. Station 6 also showed deficits of both isotopes, down to 25 m for ^{234}Th (160 ± 40 dpm m^{-2}) and 150 m for ^{210}Po (930 ± 200 dpm m^{-2}). At five stations (2, 3, 4, 7, and 8) ^{234}Th was not significantly depleted in the upper water column. On the contrary, at those stations the integrated ^{210}Po deficits in the upper water column (50–150 m) ranged from 130 ± 150 to 1640 ± 220 dpm m^{-2} . The integrated excesses of ^{210}Po observed at stations 2 (30 and 100–300 m) and 4 (15, 30–50, 150, and 400 m) exceeded the integrated deficits observed in the surface water. Finally, at stations 5 and 9 (only ^{234}Th sampling), ^{234}Th was in equilibrium with ^{238}U throughout the upper 400 m with only a few exceptions.

3.2.2. ^{234}Th and ^{210}Po Fluxes

The ^{234}Th and ^{210}Po fluxes (F_D) are attributed to scavenging of ^{234}Th and ^{210}Po onto sinking particles. The fluxes were calculated using a steady state (SS) model, neglecting advective and diffusive fluxes [Buesseler *et al.*, 1992]:

$$F_D = \lambda_D (A_P - A_D),$$

where D stands for “daughter” (^{234}Th or ^{210}Po) and P for “parent” (^{238}U or ^{210}Pb , respectively). λ_D is the decay constant of ^{234}Th (0.029 day^{-1}) or ^{210}Po (0.0050 day^{-1}), and $(A_P - A_D)$ is the integrated daughter

Table 2. ^{234}Th and ^{210}Po Export Fluxes Assuming Steady State Conditions at 25, 50, 100, and 150 m

Station	Depth (m)	^{234}Th Fluxes ($\text{dpm m}^{-2} \text{d}^{-1}$)	^{210}Po Fluxes ($\text{dpm m}^{-2} \text{d}^{-1}$)
1	25	200 ± 50	2.1 ± 0.4
	50	330 ± 60	3.9 ± 0.6
	100	230 ± 130	4.3 ± 1.0
	150	280 ± 190	1.8 ± 1.5
2	25	40 ± 50	1.6 ± 0.3
	50	70 ± 70	2.4 ± 0.4
	100	100 ± 120	1.3 ± 0.9
	150	200 ± 200	-2.2 ± 1.5
3	25	-20 ± 50	0.2 ± 0.3
	50	10 ± 70	0.8 ± 0.4
	100	20 ± 120	2.5 ± 0.7
	150	70 ± 200	4.5 ± 1.0
4	25	-70 ± 40	2.2 ± 0.6
	50	-160 ± 60	1.0 ± 0.7
	100	-160 ± 120	0.8 ± 0.8
	150	-220 ± 180	-0.4 ± 1.0
5	25	170 ± 40	nd
	50	190 ± 60	nd
	100	440 ± 110	nd
	150	660 ± 180	nd
6	25	160 ± 40	0.9 ± 0.3
	50	130 ± 60	2.1 ± 0.4
	100	180 ± 120	3.2 ± 0.7
	150	310 ± 190	4.7 ± 1.0
7	25	20 ± 50	3.4 ± 0.4
	50	90 ± 70	5.0 ± 0.5
	100	90 ± 140	7.2 ± 0.8
	150	160 ± 200	8.2 ± 1.1
8	25	0 ± 60	2.5 ± 0.4
	50	-50 ± 80	3.0 ± 0.5
	100	0 ± 120	3.7 ± 0.9
	150	20 ± 190	4.9 ± 1.1
9	25	90 ± 40	nd
	50	60 ± 70	nd
	100	-110 ± 140	nd
	150	70 ± 190	nd

nd, no available data.

deficit with respect to its parent (dpm m^{-2}). The fluxes calculated down to 25, 50, 100, and 150 m are listed in Table 2.

The ^{234}Th fluxes were negligible or very low at five out of nine stations (2, 3, 4, 7, and 8). At stations 1, 5, and 6, the ^{234}Th fluxes averaged $175 \pm 19 \text{ dpm m}^{-2} \text{d}^{-1}$ at 25 m, $210 \pm 100 \text{ dpm m}^{-2} \text{d}^{-1}$ at 50 m, $280 \pm 140 \text{ dpm m}^{-2} \text{d}^{-1}$ at 100 m, and $400 \pm 200 \text{ dpm m}^{-2} \text{d}^{-1}$ at 150 m. At station 9 the already low ^{234}Th flux at 25 m ($90 \pm 40 \text{ dpm m}^{-2} \text{d}^{-1}$) became negligible in deeper waters. The ^{210}Po fluxes were significant at all the stations, averaging $1.8 \pm 1.1 \text{ dpm m}^{-2} \text{d}^{-1}$ at 25 m, $2.6 \pm 1.5 \text{ dpm m}^{-2} \text{d}^{-1}$ at 50 m, $3 \pm 2 \text{ dpm m}^{-2} \text{d}^{-1}$ at 100 m, and $3 \pm 3 \text{ dpm m}^{-2} \text{d}^{-1}$ at 150 m. The ^{210}Po fluxes did not decrease with depth at the majority of stations (1, 3, 6, 7, and 8), whereas at stations 2 and 4 the fluxes became negligible at 100–150 m.

3.3. Particulate Fraction

Particulate ^{234}Th , ^{210}Po , ^{210}Pb , and organic carbon, and nitrogen concentrations in large particles are given in Table 3, as well as the $^{210}\text{Po}/^{210}\text{Pb}$ and molar C/N ratios.

The mean ^{234}Th activities in particles decreased with depth, ranging from $\sim 1 \text{ dpm } 100 \text{ L}^{-1}$ at 25 m to $\sim 0.3 \text{ dpm } 100 \text{ L}^{-1}$ at 150 m. ^{210}Po activities were on average $\sim 0.04 \text{ dpm } 100 \text{ L}^{-1}$ at 25 m and

$\sim 0.02 \text{ dpm } 100 \text{ L}^{-1}$ below that depth, while ^{210}Pb activities were $\sim 0.06 \text{ dpm } 100 \text{ L}^{-1}$ at 25 and 50 m, and $\sim 0.02 \text{ dpm } 100 \text{ L}^{-1}$ at 100 and 150 m. The variation between stations was large, with deviations from those means of $>50\%$ for ^{234}Th , $>80\%$ for ^{210}Po , and $>100\%$ for ^{210}Pb . Only about 0.3% of the total activity of ^{234}Th in seawater, 1.1% of ^{210}Po and 1.7% of ^{210}Pb was associated with large particles. The maximum particulate activities were found at stations 2 and 3 and the minimum at stations 7 and 8 (negligible in some instances for ^{210}Po and ^{210}Pb). The $^{210}\text{Po}/^{210}\text{Pb}$ ratios ranged from 0.2 to 6 (average: 1.2 ± 1.4 , $n = 18$), varying considerably between stations and depths.

The POC and PON concentrations were highest at 25 m, averaging 0.23 ± 0.08 and $0.028 \pm 0.011 \mu\text{mol L}^{-1}$ ($n = 8$), respectively. Below that depth the concentrations decreased by a factor of 3. The mean C/N ratio was similar at all the investigated depths, averaging 8.8 ± 1.9 ($n = 34$).

Table 4 displays the $\text{POC}/^{234}\text{Th}$ and $\text{POC}/^{210}\text{Po}$ ratios (C/Th and C/Po) at 25, 50, 100, and 150 m. The average ratios at the different horizon depths ranged from 17 to $40 \mu\text{mol C dpm}^{-1}$ for C/Th and from 300 to $1100 \mu\text{mol C dpm}^{-1}$ for C/Po. The ratios did not change significantly with depth (Kruskal-Wallis test, $P > 0.05$).

3.4. POC Fluxes

The POC fluxes were calculated multiplying the ^{234}Th and ^{210}Po fluxes derived from the SS model by the C/Th and C/Po ratios in large particles, respectively (Table 4).

The ^{234}Th -derived POC fluxes ranged from negligible to $10 \text{ mmol C m}^{-2} \text{d}^{-1}$ and averaged 1.3–4 $\text{mmol C m}^{-2} \text{d}^{-1}$ at 25, 50, 100, and 150 m. The ^{210}Po -derived POC fluxes ranged from negligible to 6.3 $\text{mmol C m}^{-2} \text{d}^{-1}$

Table 3. Particulate ^{234}Th , ^{210}Po , ^{210}Pb , Organic Carbon, and Nitrogen Concentrations, $^{210}\text{Po}/^{210}\text{Pb}$ Ratios and Molar C/N Ratios in Particles $>53 \mu\text{m}$

Station	Depth (m)	Part. ^{234}Th (dpm 100 L^{-1})	Part. ^{210}Po (dpm 100 L^{-1})	Part. ^{210}Pb (dpm 100 L^{-1})	$^{210}\text{Po}/^{210}\text{Pb}$	POC ($\mu\text{mol C L}^{-1}$)	PON ($\mu\text{mol N L}^{-1}$)	C/N
1	15	0.45 ± 0.03	0.026 ± 0.003	0.0042 ± 0.0012	6 ± 2	0.25	0.038	6.6
	50	nd	nd	nd	nd	nd	nd	nd
	90	0.335 ± 0.019	0.008 ± 0.003	0.0144 ± 0.0018	0.6 ± 0.2	0.074	0.0092	8.1
	190	0.138 ± 0.008	0.011 ± 0.002	0.0057 ± 0.0011	1.8 ± 0.5	0.034	0.0054	6.3
2	25	nd	nd	nd	nd	nd	nd	nd
	50	1.71 ± 0.12	0.032 ± 0.006	0.031 ± 0.003	1.0 ± 0.2	0.23	0.034	6.7
	100	1.86 ± 0.12	0.120 ± 0.011	0.073 ± 0.004	1.6 ± 0.2	0.12	0.020	6.3
	150	0.89 ± 0.06	0.050 ± 0.007	0.055 ± 0.004	0.91 ± 0.14	0.042	0.0068	6.1
3	25	1.63 ± 0.09	0.066 ± 0.010	0.217 ± 0.010	0.30 ± 0.05	0.27	0.033	8.1
	50	1.60 ± 0.11	0.054 ± 0.014	0.221 ± 0.011	0.24 ± 0.07	0.15	0.020	7.8
	100	0.215 ± 0.012	<0.003	0.039 ± 0.003		0.032	0.0043	7.4
4	150	0.51 ± 0.02	0.035 ± 0.006	0.040 ± 0.004	0.9 ± 0.2	0.087	0.010	8.5
	25	0.55 ± 0.03	0.025 ± 0.003	0.044 ± 0.003	0.57 ± 0.08	0.28	0.029	9.8
	50	0.47 ± 0.03	0.015 ± 0.003	0.031 ± 0.002	0.47 ± 0.12	0.036	0.0056	6.4
	100	0.276 ± 0.010	<0.003	0.0152 ± 0.0016		0.097	0.014	7.0
5	150	0.43 ± 0.02	0.007 ± 0.003	0.023 ± 0.002	0.31 ± 0.15	0.058	0.0078	7.5
	25	1.50 ± 0.10	nd	nd	nd	0.38	0.047	8.0
	50	0.88 ± 0.06	nd	nd	nd	0.14	0.016	8.5
	100	0.414 ± 0.016	nd	nd	nd	0.097	0.011	9.2
6	150	0.58 ± 0.03	nd	nd	nd	0.061	0.0075	8.2
	25	1.25 ± 0.08	0.077 ± 0.006	0.106 ± 0.005	0.73 ± 0.06	0.15	0.014	11
	50	0.250 ± 0.014	0.006 ± 0.003	0.026 ± 0.002	0.21 ± 0.12	0.025	0.0025	10
	100	0.094 ± 0.005	<0.003	0.008 ± 0.002		0.015	0.0014	10
7	150	0.096 ± 0.009	0.013 ± 0.003	0.0059 ± 0.0016	2.2 ± 0.8	0.012	0.00090	14
	25	0.42 ± 0.02	0.0126 ± 0.0018	0.0076 ± 0.0014	1.7 ± 0.4	0.23	0.023	10
	50	0.062 ± 0.007	<0.003	<0.003		0.029	0.0028	11
	100	0.061 ± 0.009	<0.003	0.0040 ± 0.0018		0.088	0.0074	12
8	150	0.078 ± 0.006	0.009 ± 0.003	<0.003		0.036	0.0029	12
	25	0.51 ± 0.02	0.009 ± 0.003	0.010 ± 0.002	0.9 ± 0.3	0.16	0.020	8.1
	50	0.286 ± 0.016	0.008 ± 0.003	0.026 ± 0.003	0.31 ± 0.13	0.049	0.0051	9.6
	100	0.133 ± 0.014	<0.003	0.012 ± 0.003		0.080	0.0070	11
9	150	0.100 ± 0.008	<0.003	0.0040 ± 0.0018		0.032	0.0040	8.2
	25	1.34 ± 0.10	nd	nd	nd	0.15	0.020	7.4
	50	0.64 ± 0.03	nd	nd	nd	0.088	0.0091	9.7
	100	0.229 ± 0.011	nd	nd	nd	0.069	0.0077	9.0
	150	0.18 ± 0.02	nd	nd	nd	0.059	0.0064	9.3

nd, no available data.

$\text{m}^{-2} \text{d}^{-1}$ and averaged $0.8\text{-}3 \text{ mmol C m}^{-2} \text{d}^{-1}$ at the same depths. The POC fluxes estimated using the two proxies were not significantly different considering all depths together, or each depth individually (Wilcoxon test, $P > 0.05$).

4. Discussion

In this study we have used two pairs of radionuclides, $^{234}\text{Th}/^{238}\text{U}$ and $^{210}\text{Po}/^{210}\text{Pb}$, as tools to estimate POC fluxes in the Eurasian Basin of the Arctic Ocean in summer 2012. Deficits of ^{234}Th and ^{210}Po are attributed to particle export, while the excesses of these radionuclides evidence their release from sinking particles by means of remineralization or particle disaggregation into the suspended pool. Their simultaneous application allows integrating a temporal scale over a span of weeks (^{234}Th mean life = 35 days) to months (^{210}Po mean life = 200 days).

4.1. $^{234}\text{Th}/^{238}\text{U}$

4.1.1. ^{234}Th Export Fluxes

^{234}Th export fluxes were calculated using a SS model because the stations were not reoccupied during the expedition. Yet in a review study Savoye *et al.* [2006] did not find significant differences between the SS and nonsteady state (NSS) models at low flux rates ($<800 \text{ dpm m}^{-2} \text{d}^{-1}$), which is the case of the present work.

Significant ^{234}Th fluxes within the upper 150 m of the water column were obtained at stations 1, 5, and 6, and at specific depths at some other stations (Table 2). The ^{234}Th fluxes ranged from negligible to 660 dpm

Table 4. Particulate C/Th and C/Po Ratios and POC Fluxes Derived From ²³⁴Th and ²¹⁰Po

Station	Depth (m)	C/Th (μmol C dpm ⁻¹)	C/Po (μmol C dpm ⁻¹)	POC Fluxes (mmol C m ⁻² d ⁻¹)	
				²³⁴ Th-Derived	²¹⁰ Po-Derived
1	15	56 ± 4	970 ± 100	7 ± 2	1.2 ± 0.4
	50	nd	nd	nd	nd
	90	22.1 ± 1.3	900 ± 400	5 ± 3	4 ± 2
	190	25.0 ± 1.5	330 ± 70	10 ± 6	0.1 ± 0.7
2	25	nd	nd	nd	nd
	50	13.2 ± 0.9	700 ± 120	0.9 ± 0.9	1.7 ± 0.4
	100	6.7 ± 0.5	104 ± 9	0.7 ± 0.8	0.13 ± 0.09
	150	4.7 ± 0.3	83 ± 12	0.9 ± 0.9	-0.19 ± 0.13
3	25	16.3 ± 0.9	400 ± 60	-0.4 ± 0.8	0.06 ± 0.14
	50	9.6 ± 0.6	280 ± 80	0.1 ± 0.7	0.23 ± 0.14
	100	14.8 ± 0.8		0 ± 2	
	150	16.9 ± 0.8	250 ± 40	1 ± 3	1.1 ± 0.3
4	25	51 ± 3	1140 ± 140	-4 ± 2	2.5 ± 0.7
	50	7.7 ± 0.4	250 ± 60	-1.2 ± 0.5	0.3 ± 0.2
	100	35.2 ± 1.3		-6 ± 4	
	150	13.6 ± 0.6	800 ± 400	-3 ± 2	-0.3 ± 0.9
5	25	25.1 ± 1.7	nd	4.3 ± 1.0	nd
	50	15.6 ± 1.0	nd	2.9 ± 0.9	nd
	100	23.5 ± 0.9	nd	10 ± 3	nd
	150	10.5 ± 0.5	nd	7 ± 2	nd
6	25	12.2 ± 0.8	197 ± 14	1.9 ± 0.5	0.18 ± 0.07
	50	10.1 ± 0.5	500 ± 200	1.3 ± 0.6	1.0 ± 0.5
	100	15.5 ± 0.8		3 ± 2	
	150	12.7 ± 1.2	90 ± 20	4 ± 2	0.44 ± 0.13
7	25	54 ± 3	1800 ± 300	1 ± 3	6.3 ± 1.1
	50	48 ± 6		4 ± 3	
	100	150 ± 20		10 ± 20	
	150	47 ± 4	390 ± 110	7 ± 9	3.2 ± 1.0
8	25	32.3 ± 1.4	1900 ± 600	0 ± 2	4.8 ± 1.6
	50	17.1 ± 1.0	600 ± 300	-0.9 ± 1.3	1.8 ± 1.3
	100	60 ± 6		0 ± 7	
	150	32 ± 3		1 ± 6	
9	25	11.2 ± 0.8	nd	1.0 ± 0.5	nd
	50	13.7 ± 0.8	nd	0.9 ± 0.9	nd
	100	30.2 ± 1.4	nd	-3 ± 4	nd
	150	32 ± 4	nd	2 ± 6	Nd

nd, no available data.

m⁻² d⁻¹, averaging 120 ± 140 dpm m⁻² d⁻¹ (n = 36). Our results are 1 order of magnitude lower than the ²³⁴Th flux average reported by *Le Moigne et al.* [2013b] for the world ocean (1200 ± 900 dpm m⁻² d⁻¹; 75–210 m; n = 421). Previous research conducted in the central Arctic, mainly during summer, has also revealed low export fluxes escaping from the ocean surface (Figure 3). *Cai et al.* [2010] reported an average of 90 ± 300 dpm m⁻² d⁻¹ (n = 26) in the most extensive study of ²³⁴Th over the central basins to date, and *Moran et al.* [1997] and *Gustafsson and Andersson* [2012] reported similar flux averages of 190 ± 140 dpm m⁻² d⁻¹ (n = 7) and 130 ± 100 dpm m⁻² d⁻¹ (n = 3), respectively. *Le Moigne et al.* [2015] reported ²³⁴Th fluxes of 140 ± 210 dpm m⁻² d⁻¹ in the ice-covered Fram Strait, which is also in line with our results. Nevertheless, other studies have reported high ²³⁴Th export fluxes (>2000 dpm m⁻² d⁻¹) at specific locations in the Canada Basin [*Ma et al.*, 2005], although they are more typical of the shelf environment [e.g., *Coppola et al.*, 2002; *Lepore et al.*, 2007] (Figure 3). Overall, the ²³⁴Th flux data presented here and the limited data available to date illustrate the central Arctic basins as deserts in terms of particle export during summer.

4.1.2. ²³⁴Th-Derived POC Export Fluxes

The mean ²³⁴Th-derived POC export fluxes measured in the upper 150 m were 3 ± 3 mmol C m⁻² d⁻¹ (n = 34), with a maximum of 10 mmol C m⁻² d⁻¹ (Table 4). At the bottom of the euphotic zone (~25 m) the fluxes ranged from negligible to 7 mmol C m⁻² d⁻¹ (average: 2 ± 2 mmol C m⁻² d⁻¹, n = 8). These results are in very good agreement with the POC fluxes measured with cylindrical sediment traps (Hydro-Bios, Kiel, Germany) deployed under the ice during periods of 24–53 h from station 1 to 9 [*Lalande et al.*, 2014]. The sediment trap results ranged from 0.4 to 9 mmol C m⁻² d⁻¹ (average: 3 ± 3 mmol C m⁻² d⁻¹, n = 9). The in situ NPP rates showed positive correlations with ²³⁴Th fluxes at 25 m (*P* < 0.05; Spearman correlation coefficient, ρ = 0.83; n = 8), ²³⁴Th-derived POC fluxes at 25 m (*P* < 0.05; ρ = 0.78; n = 7) and

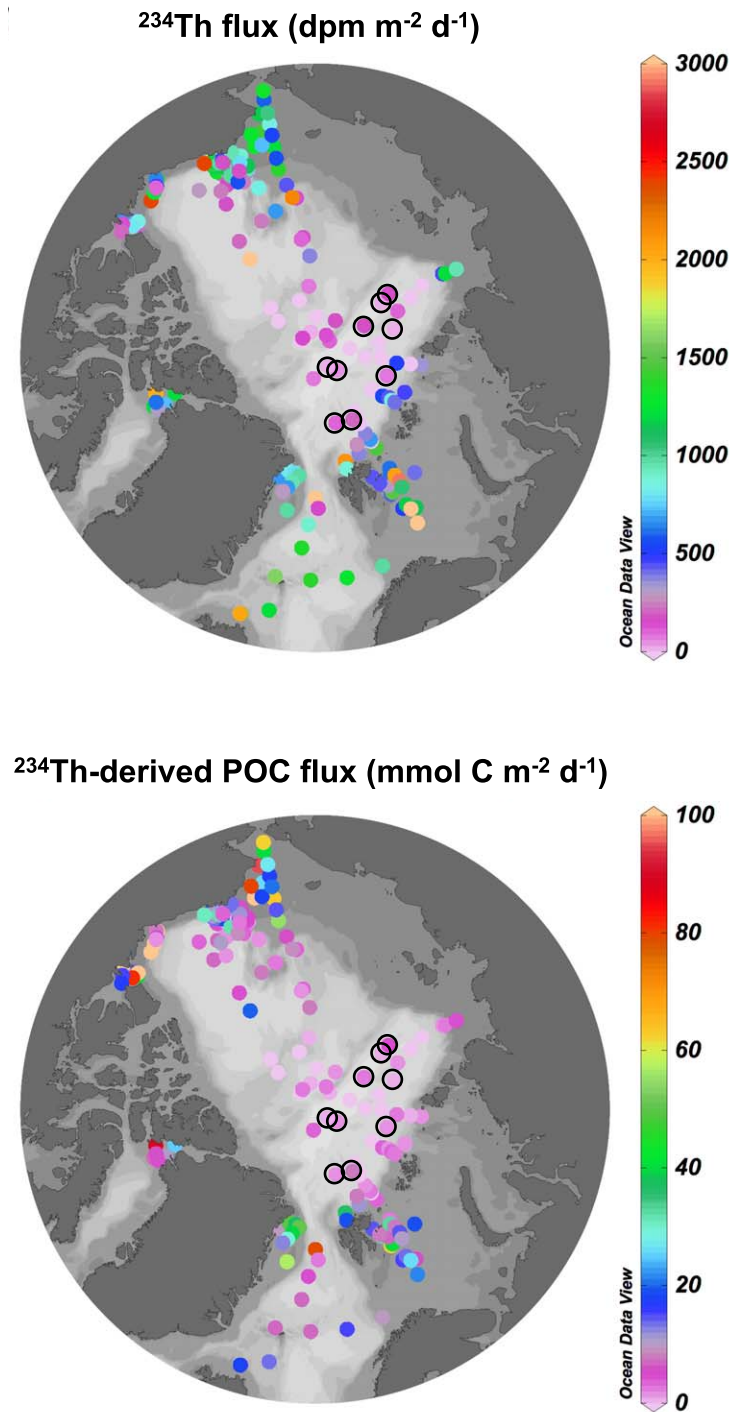


Figure 3. Compilation of ^{234}Th flux data (top) and ^{234}Th -derived POC flux data (bottom) from the Arctic Ocean (236 stations) [Cochran et al., 1995b; Moran et al., 1997, 2005; Moran and Smith, 2000; Amiel et al., 2002; Coppola et al., 2002; Baskaran et al., 2003; Chen et al., 2003; Ma et al., 2005; Trimble and Baskaran, 2005; Lepore et al., 2007; Lalande et al., 2007, 2008; Amiel and Cochran, 2008; Yu et al., 2010, 2012; Cai et al., 2010; Gustafsson and Andersson, 2012; Le Moigne et al., 2015, this study]. Black circles indicate the results obtained in this study. The depth horizon taken to calculate the POC export fluxes ranges from 25 to 200 m.

sediment trap-derived POC fluxes at 25 m ($P < 0.05$; $\rho = 0.83$; $n = 8$), which indicates enhanced particle fluxes with increasing NPP. Our results also compare well with previous literature values from sediment traps deployed at 150–175 m north of the Laptev Sea continental margin in August–September during the years 95/96 and 05/

06 ($\sim 0.5\text{--}2.5$ mmol C m⁻² d⁻¹) [Fahl and Nöthig, 2007; Lalande et al., 2009] and ²³⁴Th-derived POC fluxes in the central Arctic (Figure 3). Cai et al. [2010] documented very low POC export fluxes (average: 0.2 ± 1.0 mmol C m⁻² d⁻¹, $n = 26$) across the deep Arctic, suggesting that they were a consequence of low biological productivity. Our low POC export flux estimates are in good agreement with the low NPP observed in the present study within the ²³⁴Th time window (in situ, 1 and 2 week estimates; ≤ 5 mmol C m⁻² d⁻¹; Table 1).

4.1.3. Relationships With Phytoplankton Community

We did not find any significant relationship between the ²³⁴Th data (particulate ²³⁴Th activity, ²³⁴Th fluxes, and ²³⁴Th-derived POC fluxes) and the phytoplankton size structure at the sampling time, although two correlations were obtained with regards to the phytoplankton composition. The relative biomass of prasinophytes_1 was positively correlated with ²³⁴Th fluxes ($P < 0.05$; $\rho = 0.75$; $n = 8$) and ²³⁴Th-derived POC fluxes ($P < 0.05$; $\rho = 0.77$; $n = 7$) at 25 m. This suggests that prasinophytes_1 would have contributed significantly to vertical export fluxes during the late summer in 2012 when picoplankton, and particularly prasinophytes, were the predominant group in terms of biomass (Prasinophytes_1 and 2, Table 1). Prasinophytes are green algae that can be usually found in the eukaryotic picoplankton fraction. A molecular study by Metfies et al. [2016] corroborates the biomass dominance of picoplankton in the upper water column during our expedition and identifies the prasinophyte *Micromonas* spp. as its major constituent. Our finding is in line with recent observations that reveal that small cells are important contributors to POC export fluxes in diverse oceanic regimes [e.g., Richardson and Jackson, 2007; Lomas and Moran, 2011; Durkin et al., 2015; Mackinson et al., 2015; Puigcorb  et al., 2015]. Prasinophytes, including *Micromonas* spp., are common in the central Arctic [Booth and Horner, 1997; Sherr et al., 2003; Zhang et al., 2015], and are considered to be among the most abundant photosynthetic cells in pan-Arctic waters [Lovejoy et al., 2007]. Genetic analyses in trap samples revealed that prasinophytes contributed to downward fluxes in the Sargasso Sea [Amacher et al., 2013], but to our knowledge, this has not been observed before in Arctic waters. It is relevant to note that neither genetic nor pigment techniques inform about whether they sink as single cells or as part of other export pathways.

The pathways by which picoplankton cells can be removed from the ocean surface are fundamentally: (i) zooplankton grazing and subsequent incorporation into fecal pellets [Waite et al., 2000; Wilson and Steinberg, 2010]; (ii) adhesion into mucous nets formed by gelatinous zooplankton, such as pteropods, and later settling [Noji et al., 1997]; and (iii) inclusion into marine snow via particle aggregation, which is enhanced by transparent exopolymer particles (TEP) [Passow, 2002]. Passive sinking of fecal pellets could be a significant pathway for particle export in the central Arctic where zooplankton exert a strong grazing pressure on algae, preventing their biomass accumulation and sedimentation [Olli et al., 2007]. Indeed, the copepod food demand during our cruise was estimated to be similar to the in situ NPP rates [David et al., 2015], leaving a small fraction of algae available for direct export. Yet Lalande et al. [2014] estimated that only up to 7.5% of the POC collected by traps at 25 m consisted of fecal pellets. Trap samples also consisted of marine snow, debris, appendicularian houses, animal body parts, and very sticky material, even though their relative importance in POC content was not quantified (C. Lalande, personal communication, 2016). Copepods clearly dominated the zooplankton community with regards to abundance, whereas pteropods, ctenophores, and appendicularians, which are prone to produce mucous, represented less than 3–5% of the total zooplankton abundance either beneath the ice [David et al., 2015] or within the upper 50 m [Ehrlich, 2015]. However, ctenophores and appendicularians dominated the under-ice zooplankton biomass at some stations, which could have contributed notably to the export of mucous (C. David, personal communication, 2016). Moreover, sea-ice algal aggregates of the centric diatom *Melosira arctica* and pennate diatoms were observed at all the stations [Fern ndez-M ndez et al., 2014]. They reached abundances of up to 16 ind/m² and extraordinary sizes (mean diameter of 2.1–4.1 cm), although they showed a highly patchy distribution [Kattlein et al., 2014]. The aggregates were associated with mucous matrices that increased their stickiness and, at the same time, their predisposition to aggregation [Fern ndez-M ndez et al., 2014]. Indeed, *Melosira arctica* was intercepted using sediment traps deployed at 25 m at some stations [Lalande et al., 2014], confirming that it was part of the sinking pool. Taken all together, sea-ice algal aggregates and zooplankton-derived material might have acted as carriers of picoplankton cells from the ocean surface to depth (Figure 4b).

4.2. ²¹⁰Po/²¹⁰Pb

4.2.1. ²¹⁰Po and ²¹⁰Pb Activities

²¹⁰Po activities were lower than those of ²¹⁰Pb at every station in the upper 50–150 m, indicating export driven by sinking particles, while excess ²¹⁰Po was observed at several depths throughout the upper 400 m

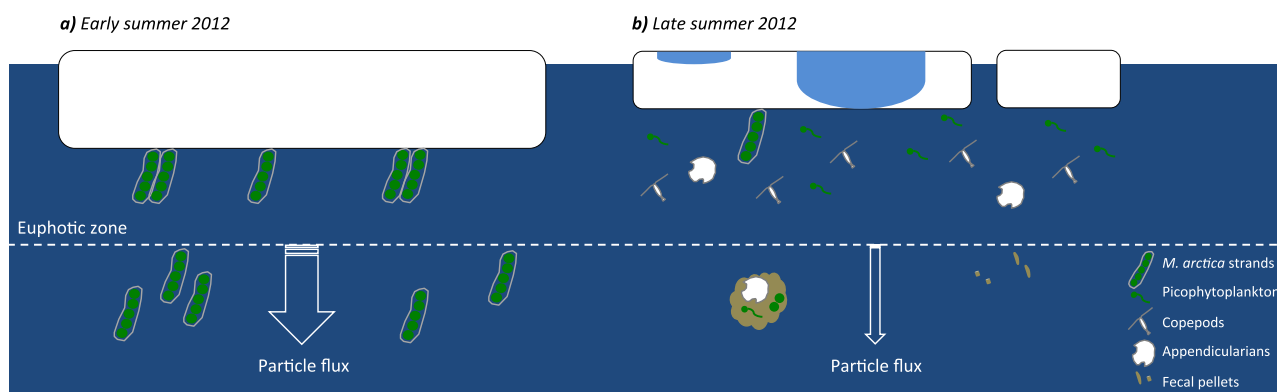


Figure 4. Scheme of the magnitude and composition of the particle fluxes in the central Arctic during the (a) early and (b) late summer in 2012 based on results from the present study and others [Boetius *et al.*, 2013; Lalande *et al.*, 2014; David *et al.*, 2015; Fernández-Méndez *et al.*, 2015] (see sections 4.1 and 4.2 for further details). Symbols are not drawn to scale.

at stations 2 and 4, suggesting remineralization or particle disaggregation (Figure 2). At stations 2 and 4, the integrated excess surpassed the integrated deficit at 150 m and below, which can be explained by (i) a previous large export event that occurred at the study sites and/or (ii) advection of waters that were enriched in ^{210}Po as consequence of a previous export event [Stewart *et al.*, 2007a]. Thus, the assumption of SS and/or neglecting the advective term would have added uncertainty to our flux estimates of ^{210}Po . We note that the ^{210}Po flux estimates are subject to be affected by NSS conditions or advection transport processes to a larger extent than the ^{234}Th flux estimates due to the longer half-life of ^{210}Po .

Very few studies have investigated the distribution of ^{210}Po and/or ^{210}Pb in the Arctic water column [Moore and Smith, 1986; Cochran *et al.*, 1995a; Smith and Ellis, 1995; Roberts *et al.*, 1997; Smith *et al.*, 2003; Lepore *et al.*, 2009; Chen *et al.*, 2012]. The ^{210}Pb and ^{210}Po activities presented here are comparable to the wide activity range reported by those studies, including shelf and basin areas.

In the Arctic, sea ice intercepts and accumulates atmospheric fluxes of chemical species, such as ^{210}Pb , during its transit through the ocean [Masqué *et al.*, 2007; Cámara-Mor *et al.*, 2011] and, therefore, sea-ice melting may increase ^{210}Pb activities in surface waters where that occurs [Roberts *et al.*, 1997; Masqué *et al.*, 2007; Chen *et al.*, 2012]. One might wonder whether sea-ice melting may significantly impact the ^{210}Po and ^{210}Pb activities in seawater and, thus, affect the use of the ^{210}Po proxy. Data on ^{210}Pb and ^{210}Po activities in entire sea-ice cores collected during the same expedition (results not shown) show that the $^{210}\text{Po}/^{210}\text{Pb}$ ratios were ≤ 0.5 , indicating ^{210}Pb enrichment in sea ice, and consistent with the dominance of first-year ice [Masqué *et al.*, 2007]. Given the inventories of both isotopes in sea-ice cores, even with complete melting of sea ice, the $^{210}\text{Po}/^{210}\text{Pb}$ ratio in the upper 25 m of the water column would have not changed or would have decreased as much as 10%. Since this change is relatively small, we are confident that the principal cause of the ^{210}Po deficit in the upper water column was its preferential removal via particle scavenging with respect to ^{210}Pb .

4.2.2. ^{210}Po Export Fluxes

The ^{210}Po export fluxes in the upper 150 m ranged from negligible to $8.2 \text{ dpm m}^{-2} \text{ d}^{-1}$, averaging $3 \pm 2 \text{ dpm m}^{-2} \text{ d}^{-1}$ ($n = 28$, Table 2). The fluxes obtained in this study are very low in comparison to other studies conducted in other regions of the world ocean [Shimmield *et al.*, 1995; Kim and Church, 2001; Friedrich and Rutgers van der Loeff, 2002; Murray *et al.*, 2005; Stewart *et al.*, 2007a; Buesseler *et al.*, 2008; Verdeny *et al.*, 2008; Le Moigne *et al.*, 2013a], which reported fluxes from 5 to $>100 \text{ dpm m}^{-2} \text{ d}^{-1}$. However, ^{210}Po fluxes were significant at every station and at most of the investigated depths, in contrast to ^{234}Th fluxes, which were only measurable throughout the upper 150 m at three stations (Table 2). Given the half-lives of both tracers, ^{210}Po would track particle export for the entire productive season, whereas ^{234}Th distribution misses events that occurred >1 month before sampling. Thus, the more common ^{210}Po depletion than that of ^{234}Th in the upper water column suggests that the magnitude of the particle export fluxes was more important before July/August 2012 than in the weeks prior to and during the sampling (Figure 4).

Boetius *et al.* [2013] revealed the presence of vast deposits of sea-ice algal aggregates on the seafloor at the majority of the stations, which would have been exported from the ocean surface earlier in the season, particularly before June at stations 4–6 as suggested by the large body size and fecundity of the deep-sea

holothurians that fed on the algae. The aggregates were mainly composed of *Melosira arctica* [Boetius *et al.*, 2013] that can form long strands hanging from the ice bottom, sometimes up to 6 m long [Melnikov and Bondarchuk, 1987], allowing a rapid sinking throughout the water column once detached. Boetius *et al.* [2013] estimated that algae covered up to 10% of the seafloor by means of high-resolution pictures, accounting for a median of $750 \text{ mmol C m}^{-2}$ ($\pm 50\%$). This POC inventory of algae was obtained by applying a cell volume to carbon ratio ($0.15 \text{ pg C } \mu\text{m}^3$) and a fixed thickness of the algal cover (1 cm). This supports the ^{210}Po evidence that the peak of export in the study area occurred in early summer and sheds light on the composition of a major part of the sinking pool (Figure 4a). It was estimated that diatoms were responsible for at least 45% of the total primary production in 2012 [Boetius *et al.*, 2013], indicating that the phytoplankton community varied over the productive season, since diatoms did not contribute much to the Chl-*a* biomass during our cruise ($\sim 20\%$, Table 1), when surface waters were silicate-depleted in most of the study area. Previous studies with sediment traps also revealed that highest fluxes in the central Arctic occur mainly in June–August when ice algae appear to be significant contributors to the export fluxes [Fahl and Nöthig, 2007; Lalonde *et al.*, 2009].

4.2.3. Relationships With Sea-Ice Conditions

There were significant relationships between the sea-ice conditions and the ^{210}Po -derived fluxes. Sea-ice concentration was positively correlated with both ^{210}Po fluxes ($P < 0.01$; $\rho = 0.92$; $n = 7$) and ^{210}Po -derived POC fluxes ($P < 0.05$; $\rho = 0.91$; $n = 6$) at 25 m. Indeed, the stations located north of 87°N and covered by multiyear ice (stations 7 and 8) showed the strongest depletion of ^{210}Po within the upper 400 m (Figure 2), and the highest annual NPP rates (Table 1) and seafloor algal coverage [Boetius *et al.*, 2013]. This suggests that primary production and particle export were more important under heavy sea-ice conditions than under partially ice-covered stations and first-year ice, also suggesting that ^{210}Po tracked, to some extent, the massive algal export that occurred earlier in 2012. On the contrary, at stations with heavy sea-ice conditions we found the minimum in situ NPP rates (Table 1) and ^{234}Th in equilibrium with ^{238}U throughout the upper water column (Figure 2), indicating low or negligible primary production and particle export fluxes during the late summer.

The results presented here, combined with those from Boetius *et al.* [2013], show that the central Arctic underwent significant changes during the productive season in terms of primary production, phytoplankton composition, and export fluxes during the record low of sea ice in 2012. This has implications for the use of ^{210}Po as a tracer: the depth distribution of total ^{210}Po activity likely changed with time (NSS conditions) and the sinking material collected during the survey probably did not cause the observed ^{210}Po depletion in the upper water column. Actually, ^{210}Po activities in large particles collected at the time of sampling were inversely correlated with ^{210}Po export fluxes at 25 m ($P < 0.05$; $\rho = -0.89$; $n = 6$). The SS model would tend to smooth out episodic export events that took place earlier in the season, and hence underestimate the mean ^{210}Po fluxes and ^{210}Po -derived POC fluxes on a seasonal scale. On the other hand, we measured C/Po ratios in particles that fall in the upper range of previous values (see review by Verdeny *et al.* [2009]). Stewart *et al.* [2007a] showed that C/Po ratios varied according to the sinking material composition as follows: degraded material > fresh phytoplankton > fecal pellets. In some instances we also found particulate $^{210}\text{Po}/^{210}\text{Pb}$ ratios below one (Table 3), which is inconsistent with the ^{210}Po deficiency observed in surface waters. Particle types that may potentially explain low $^{210}\text{Po}/^{210}\text{Pb}$ ratios could be: those remineralized by chemical and biological processes [Stewart *et al.*, 2007b]; fecal material [Stewart *et al.*, 2005; Rodriguez y Baena *et al.*, 2017]; picoplankton aggregates [Stewart *et al.*, 2010]; substrates rich in transparent exopolymer particles [Quigley *et al.*, 2002]; and sea-ice drafted material incorporated over the shelves, such as sea-ice sediments (SIS), and enriched in ^{210}Pb via atmospheric input ($^{210}\text{Po}/^{210}\text{Pb}$ ratios in SIS collected during the expedition were ≤ 1 , results not shown). If the sinking pool responsible for ^{210}Po scavenging had different C/Po ratios with respect to that collected at the sampling time, the ^{210}Po -derived POC fluxes obtained in this study would not be fully representative of the fluxes that occurred in the productive season in 2012.

4.3. Export Efficiency

We have estimated the export efficiency by dividing the POC export fluxes derived from ^{234}Th and ^{210}Po at 25 m (i.e., \sim bottom of the euphotic zone) by different estimates of NPP that encompass daily, weekly, and annual time scales (Table 5).

Table 5. Export Efficiency According to the ^{234}Th and ^{210}Po Proxies Estimated Using Different Estimates of Daily NPP (In Situ, One Week, and Two Weeks Before Sampling and Annual New Primary Production; See Text for Further Details)

Station	Export Efficiency (%)			
	In Situ	One Week	Two Weeks	Annual
<i>Th Proxy</i>				
1 ^a	>100	>100	>100	>100
2 ^b	30 ± 40	40 ± 40	30 ± 40	20 ± 20
3	0	0	0	0
4	0	0	0	0
5	90 ± 20	>100	>100	77 ± 18
6	80 ± 20	100 ± 30	80 ± 20	60 ± 17
7	>100	>100	>100	10 ± 20
8	0	0	0	0
9	nd	nd	nd	13 ± 6
<i>Po Proxy</i>				
1 ^a	37 ± 12	53 ± 17	50 ± 16	37 ± 12
2 ^b	64 ± 16	74 ± 19	67 ± 17	36 ± 9
3	5 ± 11	3 ± 6	3 ± 6	3 ± 7
4	>100	70 ± 20	80 ± 20	90 ± 30
5	nd	nd	nd	nd
6	8 ± 3	9 ± 4	8 ± 3	6 ± 2
7	>100	>100	>100	53 ± 9
8	>100	>100	>100	48 ± 16
9	nd	nd	nd	nd

^aPOC fluxes were measured at 15 m instead of 25 m.

^bPOC fluxes were measured at 50 m instead of 25 m.

The values in italics have relative uncertainties $\geq 100\%$.

nd, no available data.

Considering the in situ NPP rates, the export efficiencies varied widely over the study site, from 0 to $>100\%$, averaging $50 \pm 50\%$ ($n = 8$) and $60 \pm 40\%$ ($n = 7$) for the ^{234}Th and ^{210}Po proxies, respectively. The export efficiencies calculated using the fluxes measured with sediment traps [Lalande *et al.*, 2014] was $>100\%$ at six out of eight stations. Export efficiencies over 100% suggest that primary production that occurred earlier in the season contributed to the export fluxes measured (i.e., temporal decoupling between production and export). In order to cover longer time scales of NPP, we have also used estimates that integrate 1 and 2 weeks before sampling and the entire productive season (see section 3.1.2). The increase in daily NPP observed between the in situ and the weekly estimates at stations 3, 4, 7, and 8, only changed significantly the export efficiency at station 4 (^{210}Po proxy), obtaining estimates of $\sim 70\%$ (Table 5). Export efficiencies over 100% were still observed in several instances, indicating that the lag between production and

export was longer than 2 weeks. On the contrary, the export efficiencies decreased by about 40% when applying the annual NPP estimates (^{234}Th : $30 \pm 40\%$, $n = 9$; ^{210}Po : $40 \pm 30\%$, $n = 7$) and were mostly below 100%, except for ^{234}Th at station 1. In contrast to ^{234}Th , ^{210}Po fluxes and ^{210}Po -derived POC fluxes at 25 m

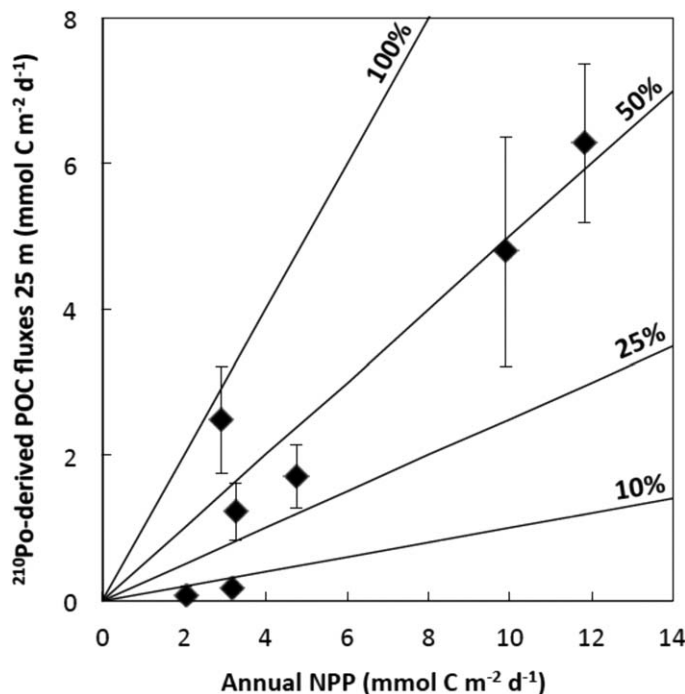


Figure 5. ^{210}Po -derived POC export fluxes at 25 m versus annual new primary production reported in Fernández-Méndez *et al.* [2015]. Solid lines indicate the export efficiency.

showed a positive correlation with the integrated deficits of nitrate found in the upper water column [Fernández-Méndez *et al.*, 2015] ($P < 0.05$; $\rho = 0.83$; $n = 6$), which are used to estimate the annual new NPP rates [e.g., Codispoti *et al.*, 2013]. This confirms that the ^{210}Po proxy covered the productive season better than ^{234}Th and suggests that consumption of nitrate resulted in the increase in export production. Thus, the ^{210}Po -derived POC fluxes and annual NPP estimates can be useful to assess the seasonal strength of the biological pump, allowing to overcome the temporal decoupling between production and export, which is especially long in Arctic waters according to a global biogeochemical model presented by Henson *et al.* [2015].

The export efficiencies based on the annual NPP and the ^{210}Po -

derived POC fluxes are illustrated in Figure 5. Only two locations showed export efficiencies <10% (stations 3 and 6; Table 5), which are those typically found in the world ocean [Buesseler, 1998]. In this line, Cai *et al.* [2010] reported export efficiencies <6% in the central Arctic using historical measurements of primary production. In contrast, export efficiencies >30% (average: $50 \pm 20\%$, $n = 5$) were found at the other stations, which are in good agreement with those reported by Gustafsson and Andersson [2012] in the Eurasian Basin (average: $34 \pm 8\%$, $n = 3$) and Chen *et al.* [2003] in the Canada Basin (26%, $n = 1$) applying ^{234}Th -derived POC fluxes and in situ NPP rates. Our estimates are also similar to the ^{234}Th -derived export efficiencies of ~30–40% reported for Chukchi shelf, slope, and basin stations in summer [Moran *et al.*, 2005; Lepore *et al.*, 2007]. Although only a limited set of observations of export efficiency is available in the central Arctic, overall they point to high export efficiencies as also indicated by Henson *et al.* [2015]. The assessment of the export efficiency in the central Arctic deserves more attention to better understand its role as an export regime in a climate change framework. Observations of strong aggregation and rapid algal falls in the central Arctic [Boetius *et al.*, 2013; Katlein *et al.*, 2014] suggest an export system that works differently than in most of the world ocean.

5. Conclusions

We have used concurrently the $^{234}\text{Th}/^{238}\text{U}$ and $^{210}\text{Po}/^{210}\text{Pb}$ proxies to estimate POC fluxes in the central Arctic during the record sea-ice minimum in 2012. The main findings of the present work are:

1. ^{234}Th reveals that POC fluxes at the bottom of the euphotic zone were very low ($2 \pm 2 \text{ mmol C m}^{-2} \text{ d}^{-1}$) in August/September, which is in good agreement with results obtained using sediment traps ($3 \pm 3 \text{ mmol C m}^{-2} \text{ d}^{-1}$) deployed at the same locations [Lalande *et al.*, 2014]. The positive relationships found between prasinophytes_1 and ^{234}Th and ^{234}Th -derived POC fluxes suggest that picoplankton contributed significantly to downward fluxes in late summer.
2. In contrast to ^{234}Th , the upper water column was depleted in ^{210}Po over the entire study area, indicating that particle export fluxes were higher before July/August than in the weeks prior to and during the survey.
3. The positive relationships obtained between sea-ice concentration and ^{210}Po and ^{210}Po -derived POC fluxes show that particle sinking was greater under heavy sea-ice conditions than under partially ice-covered areas. Further, the strongest ^{210}Po deficits in the water column coincided with the highest sea-floor coverage of algae reported by Boetius *et al.* [2013], suggesting that ^{210}Po tracked, to some extent, the massive algal export that occurred earlier in the season.
4. Although the POC fluxes were low, a large fraction of primary production (>30%) was exported at the base of the euphotic zone in most of the study area, according to ^{210}Po -derived POC fluxes and annual NPP estimates. Seasonal estimates of primary production and export would be very helpful in characterizing the role of the Arctic biological pump in the context of climate change.

We encourage future studies applying radionuclide proxies to consider NSS conditions and follow the trend of C/Th and C/Po ratios with time to better constrain the POC fluxes in the Arctic. Further, the simultaneous use of sediment traps would allow the determination of the particle flux composition, which has been pointed out as a crucial factor shaping the biological pump efficiency [e.g., Mackinson *et al.*, 2015; Puigcorb e *et al.*, 2016; Roca-Mart ı *et al.*, 2016].

References

- Amacher, J., S. Neuer, and M. Lomas (2013), DNA-based molecular fingerprinting of eukaryotic protists and cyanobacteria contributing to sinking particle flux at the Bermuda Atlantic time-series study, *Deep-Sea Res., Part II*, 93, 71–83, doi:10.1016/j.dsr2.2013.01.001.
- Amiel, D., and J. K. Cochran (2008), Terrestrial and marine POC fluxes derived from ^{234}Th distributions and $\delta^{13}\text{C}$ measurements on the Mackenzie Shelf, *J. Geophys. Res.*, 113, C03S06, doi:10.1029/2007JC004260.
- Amiel, D., J. K. Cochran, and D. J. Hirschberg (2002), $^{234}\text{Th}/^{238}\text{U}$ disequilibrium as an indicator of the seasonal export flux of particulate organic carbon in the North Water, *Deep-Sea Res., Part II*, 49(22–23), 5191–5209, doi:10.1016/S0967-0645(02)00185-6.
- Anderson, L. G., and R. W. Macdonald (2015), Observing the Arctic Ocean carbon cycle in a changing environment, *Polar Res.*, 34, 26891, doi:10.3402/polar.v34.26891.
- Arrigo, K. R., and G. L. van Dijken (2015), Continued increases in Arctic Ocean primary production, *Prog. Oceanogr.*, 136, 60–70, doi:10.1016/j.pocean.2015.05.002.
- Arrigo, K. R., et al. (2012), Massive phytoplankton blooms under Arctic sea ice, *Science*, 336(6087), 1408, doi:10.1126/science.1215065.
- Barlow, R., D. Cummings, and S. Gibb (1997), Improved resolution of mono- and divinyl chlorophylls a and b and zeaxanthin and lutein in phytoplankton extracts using reverse phase C-8 HPLC, *Mar. Ecol. Prog. Ser.*, 161, 303–307, doi:10.3354/meps161303.

Acknowledgments

We wish to acknowledge the support of the crew and scientific party of the R/V Polarstern ARK-XXVII/3 expedition. We are very grateful to I. Stimac for her assistance with the cruise preparation and ICPMS analyses, and D. Scholz for his support on board especially with the in situ pump deployments. Sea-ice concentration data for September 2012 were obtained from <http://www.meereisportal.de> (grant REKLIM-2013-04) [Spreen *et al.*, 2008]. The authors acknowledge C. Lalande, C. David, H. Flores, E.-M. N othig, M. Nicolaus, and B. Rabe for providing valuable comments on earlier drafts. The manuscript was improved by comments from two anonymous reviewers. This project was partly supported by the Ministerio de Ciencia e Innovaci on (CTM2011-28452, Spain) and the Generalitat de Catalunya to the research group MERS (2014 SGR-1356). M.R.-M. and V.P. were supported by Spanish PhD fellowships (AP2010-2510 and AP2009-4733, respectively). The data used in this manuscript are listed in tables or are available at <http://doi.pangaea.de/10.1594/PAN-GAEA.858790>.

- Baskaran, M., P. W. Swarzenski, and D. Porcelli (2003), Role of colloidal material in the removal of ^{234}Th in the Canada basin of the Arctic Ocean, *Deep-Sea Res., Part I*, 50(10–11), 1353–1373, doi:10.1016/S0967-0637(03)00140-7.
- Bigdare, R. R. (1991), Analysis of algal chlorophylls and carotenoids, in *Marine Particles: Analysis and Characterization*, edited by D. C. Hurd and D. W. Spencer, pp. 119–123, AGU, Washington, D. C.
- Boetius, A. (2013), The expedition of the research vessel “Polarstern” to the Arctic in 2012 (ARK-XXVII/3), in *Reports on Polar and Marine Research, Rep. 663*, 166 p., Alfred Wegener Inst. for Polar and Mar. Res., Bremerhaven, Germany.
- Boetius, A., et al. (2013), Export of algal biomass from the melting Arctic sea ice, *Science*, 339(6126), 1430–1432, doi:10.1126/science.1231346.
- Booth, B. C., and R. A. Horner (1997), Microalgae on the arctic ocean section, 1994: Species abundance and biomass, *Deep-Sea Res., Part II*, 44(8), 1607–1622, doi:10.1016/S0967-0645(97)00057-X.
- Buesseler, K. O. (1998), The decoupling of production and particulate export in the surface ocean, *Global Biogeochem. Cycles*, 12(2), 297–310, doi:10.1029/97GB03366.
- Buesseler, K. O., and P. Boyd (2009), Shedding light on processes that control particle export and flux attenuation in the twilight zone of the open ocean, *Limnol. Oceanogr.*, 54(4), 1210–1232, doi:10.4319/lo.2009.54.4.1210.
- Buesseler, K. O., M. P. Bacon, J. K. Cochran, and H. D. Livingston (1992), Carbon and nitrogen export during the JGOFS North Atlantic Bloom experiment estimated from ^{234}Th : ^{238}U disequilibria, *Deep-Sea Res., Part I*, 39(7–8), 1115–1137, doi:10.1016/0198-0149(92)90060-7.
- Buesseler, K. O., C. Benitez-Nelson, M. M. Rutgers van der Loeff, J. Andrews, L. Ball, G. Crossin, and M. A. Charette (2001), An intercomparison of small- and large-volume techniques for thorium-234 in seawater, *Mar. Chem.*, 74(1), 15–28, doi:10.1016/S0304-4203(00)00092-X.
- Buesseler, K. O., C. Lamborg, P. Cai, R. Escoube, R. Johnson, S. Pike, P. Masqué, D. McGillicuddy, and E. Verdeny (2008), Particle fluxes associated with mesoscale eddies in the Sargasso Sea, *Deep-Sea Res., Part II*, 55(10–13), 1426–1444, doi:10.1016/j.dsr2.2008.02.007.
- Cai, P., M. M. Rutgers van der Loeff, I. Stimač, E.-M. Nöthig, K. Lepore, and S. B. Moran (2010), Low export flux of particulate organic carbon in the central Arctic Ocean as revealed by ^{234}Th : ^{238}U disequilibrium, *J. Geophys. Res.*, 115, C10037, doi:10.1029/2009JC005595.
- Cámara-Mor, P., P. Masqué, J. García-Orellana, S. Kern, J. K. Cochran, and C. Hanfland (2011), Interception of atmospheric fluxes by Arctic sea ice: Evidence from cosmogenic ^7Be , *J. Geophys. Res.*, 116, C12041, doi:10.1029/2010JC006847.
- Chen, M., Y. Huang, P. Cai, and L. Guo (2003), Particulate organic carbon export fluxes in the Canada Basin and Bering Sea as derived from ^{234}Th / ^{238}U disequilibria, *ARCTIC*, 56(1), 32–44, doi:10.14430/arctic600.
- Chen, M., Q. Ma, L. Guo, Y. Qiu, Y. Li, and W. Yang (2012), Importance of lateral transport processes to ^{210}Pb budget in the eastern Chukchi Sea during summer 2003, *Deep-Sea Res., Part II*, 81–84, 53–62, doi:10.1016/j.dsr2.2012.03.011.
- Cochran, J. K., D. J. Hirschberg, H. D. Livingston, K. O. Buesseler, and R. M. Key (1995a), Natural and anthropogenic radionuclide distributions in the Nansen Basin, Arctic Ocean: Scavenging rates and circulation timescales, *Deep-Sea Res., Part II*, 42(6), 1495–1517, doi:10.1016/0967-0645(95)00051-8.
- Cochran, J. K., C. Barnes, D. Achman, and D. J. Hirschberg (1995b), Thorium-234/Uranium-238 disequilibrium as an indicator of scavenging rates and particulate organic carbon fluxes in the Northeast Water Polynya, Greenland, *J. Geophys. Res.*, 100(C3), 4399–4410, doi:10.1029/94JC01954.
- Codispoti, L. A. A., V. Kelly, A. Thessen, P. Matrai, S. Suttles, V. Hill, M. Steele, and B. Light (2013), Synthesis of primary production in the Arctic Ocean: III. Nitrate and phosphate based estimates of net community production, *Prog. Oceanogr.*, 110, 126–150, doi:10.1016/j.pocean.2012.11.006.
- Coppola, L., M. Roy-Barman, P. Wassmann, S. Mulsow, and C. Jeandel (2002), Calibration of sediment traps and particulate organic carbon export using ^{234}Th in the Barents Sea, *Mar. Chem.*, 80(1), 11–26, doi:10.1016/S0304-4203(02)00071-3.
- David, C., B. Lange, B. Rabe, and H. Flores (2015), Community structure of under-ice fauna in the Eurasian central Arctic Ocean in relation to environmental properties of sea-ice habitats, *Mar. Ecol. Prog. Ser.*, 522, 15–32.
- Durkin, C. A., M. L. Estapa, and K. O. Buesseler (2015), Observations of carbon export by small sinking particles in the upper mesopelagic, *Mar. Chem.*, 175, 72–81, doi:10.1016/j.marchem.2015.02.011.
- Ehrlich, J. (2015), Diversity and distribution of high-Arctic zooplankton in the Eurasian Basin in late summer 2012, MS thesis, Alfred Wegener Inst., Univ. of Hamburg, Hamburg, Germany.
- Fahl, K., and E.-M. Nöthig (2007), Lithogenic and biogenic particle fluxes on the Lomonosov Ridge (central Arctic Ocean) and their relevance for sediment accumulation: Vertical vs. lateral transport, *Deep-Sea Res. Part I*, 54(8), 1256–1272, doi:10.1016/j.dsr.2007.04.014.
- Falkowski, P. G., R. T. Barber, and V. Smetacek (1998), Biogeochemical controls and feedbacks on ocean primary production, *Science*, 281(5374), 200–206, doi:10.1126/science.281.5374.200.
- Fernández-Méndez, M., F. Wenzhöfer, I. Peeken, H. L. Sørensen, R. N. Glud, and A. Boetius (2014), Composition, buoyancy regulation and fate of ice algal aggregates in the Central Arctic Ocean, *PLoS One*, 9(9), e107452, doi:10.1371/journal.pone.0107452.
- Fernández-Méndez, M., C. Katlein, B. Rabe, M. Nicolaus, I. Peeken, K. Bakker, H. Flores, and A. Boetius (2015), Photosynthetic production in the central Arctic Ocean during the record sea-ice minimum in 2012, *Biogeosciences*, 12(11), 3525–3549, doi:10.5194/bg-12-3525-2015.
- Fleer, A. P., and M. P. Bacon (1984), Determination of ^{210}Pb and ^{210}Po in seawater and marine particulate matter, *Nucl. Instrum. Methods Phys. Res.*, 223(2–3), 243–249, doi:10.1016/0167-5087(84)90655-0.
- Flynn, W. W. (1968), The determination of low levels of polonium-210 in environmental materials., *Anal. Chim. Acta*, 43(2), 221–227.
- Fortier, M., L. Fortier, C. Michiel, and L. Legendre (2002), Climatic and biological forcing of the vertical flux of biogenic particles under seasonal Arctic sea ice, *Mar. Ecol. Prog. Ser.*, 225, 1–16, doi:10.3354/meps225001.
- Friedrich, J., and M. M. Rutgers van der Loeff (2002), A two-tracer (^{210}Po - ^{234}Th) approach to distinguish organic carbon and biogenic silica export flux in the Antarctic Circumpolar Current, *Deep-Sea Res., Part I*, 49(1), 101–120, doi:10.1016/S0967-0637(01)00045-0.
- Gosselin, M., M. Levasseur, P. A. Wheeler, R. A. Horner, and B. C. Booth (1997), New measurements of phytoplankton and ice algal production in the Arctic Ocean, *Deep-Sea Res., Part II*, 44(8), 1623–1644, doi:10.1016/S0967-0645(97)00054-4.
- Gradinger, R., C. Friedrich, and M. Spindler (1999), Abundance, biomass and composition of the sea ice biota of the Greenland Sea pack ice, *Deep-Sea Res., Part II*, 46(6–7), 1457–1472, doi:10.1016/S0967-0645(99)00030-2.
- Gruber, N., et al. (2009), Oceanic sources, sinks, and transport of atmospheric CO_2 , *Global Biogeochem. Cycles*, 23, GB1005, doi:10.1029/2008GB003349.
- Gustafsson, Ö., and P. S. Andersson (2012), ^{234}Th -derived surface export fluxes of POC from the Northern Barents Sea and the Eurasian sector of the Central Arctic Ocean, *Deep-Sea Res., Part I*, 68, 1–11, doi:10.1016/j.dsr.2012.05.014.
- Haas, C., A. Pfaffling, S. Hendricks, L. Rabenstein, J.-L. Etienne, and I. Rigor (2008), Reduced ice thickness in Arctic Transpolar Drift favors rapid ice retreat, *Geophys. Res. Lett.*, 35, L17501, doi:10.1029/2008GL034457.
- Henson, S. A., A. Yool, and R. Sanders (2015), Variability in efficiency of particulate organic carbon export: A model study, *Global Biogeochem. Cycles*, 29(1), 33–45, doi:10.1002/2014GB004965.

- Higgins, H. W., S. W. Wright, and L. Schlüter (2011), Quantitative interpretation of chemotaxonomic pigment data, in *Phytoplankton Pigments. Characterization, Chemotaxonomy and Applications in Oceanography*, edited by S. Roy, C. Llewellyn, E. S. Egeland, and G. Johnsen, pp. 257–313, Cambridge Univ. Press, Cambridge, U. K.
- Hirata, T., et al. (2011), Synoptic relationships between surface Chlorophyll-*a* and diagnostic pigments specific to phytoplankton functional types, *Biogeosciences*, 8(2), 311–327, doi:10.5194/bg-8-311-2011.
- Honjo, S., R. A. Krishfield, T. I. Eglinton, S. J. Manganini, J. N. Kemp, K. Doherty, J. Hwang, T. K. McKee, and T. Takizawa (2010), Biological pump processes in the cryopelagic and hemipelagic Arctic Ocean: Canada Basin and Chukchi Rise, *Prog. Oceanogr.*, 85(3–4), 137–170, doi:10.1016/j.pocean.2010.02.009.
- Jeffrey, S. W., R. F. C. Mantoura, and T. Bjørnland (1997), Data for the identification of 47 key phytoplankton pigments, in *Phytoplankton Pigments in Oceanography: Guidelines to Modern Methods*, edited by S. W. Jeffrey, R. F. C. Mantoura, and S. W. Wright, pp. 449–559, Cambridge Univ. Press, Paris.
- Katlein, C., M. Fernández-Méndez, F. Wenzhöfer, and M. Nicolaus (2014), Distribution of algal aggregates under summer sea ice in the Central Arctic, *Polar Biol.*, 38(5), 719–731, doi:10.1007/s00300-014-1634-3.
- Kilias, E., C. Wolf, E.-M. Nöthig, I. Peeken, and K. Metfies (2013), Protist distribution in the Western Fram Strait in summer 2010 based on 454-pyrosequencing of 18S rDNA, *J. Phycol.*, 49(5), 996–1010, doi:10.1111/jpy.12109.
- Kim, G., and T. M. Church (2001), Seasonal biogeochemical fluxes of ²³⁴Th and ²¹⁰Po in the Upper Sargasso Sea: Influence from atmospheric iron deposition, *Global Biogeochem. Cycles*, 15(3), 651–661, doi:10.1029/2000GB001313.
- Knap, A., A. Michaels, A. Close, H. Ducklow, and A. Dickson (1996), Protocols for the Joint Global Ocean Flux Study (JGOFS) core measurements, *JGOFS Rep.* 19, 210 pp., Reprint of the IOC Manuals and Guides No. 29, UNESCO 1994.
- Lalande, C., K. Lepore, L. W. Cooper, J. M. Grebmeier, and S. B. Moran (2007), Export fluxes of particulate organic carbon in the Chukchi Sea: A comparative study using ²³⁴Th/²³⁸U disequilibria and drifting sediment traps, *Mar. Chem.*, 103(1–2), 185–196, doi:10.1016/j.marchem.2006.07.004.
- Lalande, C., S. B. Moran, P. Wassmann, J. M. Grebmeier, and L. W. Cooper (2008), ²³⁴Th-derived particulate organic carbon fluxes in the northern Barents Sea with comparison to drifting sediment trap fluxes, *J. Mar. Syst.*, 73(1–2), 103–113, doi:10.1016/j.jmarsys.2007.09.004.
- Lalande, C., A. Forest, D. G. Barber, Y. Gratton, and L. Fortier (2009), Variability in the annual cycle of vertical particulate organic carbon export on Arctic shelves: Contrasting the Laptev Sea, Northern Baffin Bay and the Beaufort Sea, *Cont. Shelf Res.*, 29(17), 2157–2165, doi:10.1016/j.csr.2009.08.009.
- Lalande, C., E.-M. Nöthig, R. Somavilla, E. Bauerfeind, V. Shevchenko, and Y. Okolodkov (2014), Variability in under-ice export fluxes of biogenic matter in the Arctic Ocean, *Global Biogeochem. Cycles*, 28(5), 571–583, doi:10.1002/2013GB004735.
- Lee, S. H., D. Stockwell, and T. E. Whitledge (2010), Uptake rates of dissolved inorganic carbon and nitrogen by under-ice phytoplankton in the Canada Basin in summer 2005, *Polar Biol.*, 33(8), 1027–1036, doi:10.1007/s00300-010-0781-4.
- Le Fouest, V., M. Babin, and J.-É. Tremblay (2013), The fate of riverine nutrients on Arctic shelves, *Biogeosciences*, 10, 3661–3677, doi:10.5194/bg-10-3661-2013.
- Le Moigne, F. A. C., M. Villa-Alfageme, R. J. Sanders, C. Marsay, S. Henson, and R. García-Tenorio (2013a), Export of organic carbon and biominerals derived from ²³⁴Th and ²¹⁰Po at the Porcupine Abyssal Plain, *Deep-Sea Res., Part I*, 72, 88–101, doi:10.1016/j.dsr.2012.10.010.
- Le Moigne, F. A. C., S. A. Henson, R. J. Sanders, and E. Madsen (2013b), Global database of surface ocean particulate organic carbon export fluxes diagnosed from the ²³⁴Th technique, *Earth Syst. Sci. Data*, 5(2), 295–304, doi:10.5194/essd-5-295-2013.
- Le Moigne, F. A. C., et al. (2015), Carbon export efficiency and phytoplankton community composition in the Atlantic sector of the Arctic Ocean, *J. Geophys. Res. Oceans*, 120, 3896–3912, doi:10.1002/2015JC010700.
- Lepore, K., et al. (2007), Seasonal and interannual changes in particulate organic carbon export and deposition in the Chukchi Sea, *J. Geophys. Res.*, 112, C10024, doi:10.1029/2006JC003555.
- Lepore, K., S. B. Moran, and J. N. Smith (2009), ²¹⁰Pb as a tracer of shelf–basin transport and sediment focusing in the Chukchi Sea, *Deep-Sea Res., Part II*, 56(17), 1305–1315, doi:10.1016/j.dsr2.2008.10.021.
- Li, W. K. W., F. A. McLaughlin, C. Lovejoy, and E. C. Carmack (2009), Smallest algae thrive as the Arctic Ocean freshens, *Science*, 326(5952), 539, doi:10.1126/science.1179798.
- Lomas, M. W., and S. B. Moran (2011), Evidence for aggregation and export of cyanobacteria and nano-eukaryotes from the Sargasso Sea euphotic zone, *Biogeosciences*, 8(1), 203–216, doi:10.5194/bg-8-203-2011.
- Lovejoy, C., W. F. Vincent, S. Bonilla, S. Roy, M.-J. Martineau, R. Terrado, M. Potvin, R. Massana, and C. Pedrós-Alió (2007), Distribution, phylogeny, and growth of cold-adapted picoprochlorophytes in Arctic seas, *J. Phycol.*, 43(1), 78–89, doi:10.1111/j.1529-8817.2006.00310.x.
- Ma, Q., M. Chen, Y. Qiu, and Y. Li (2005), Regional estimates of POC export flux derived from thorium-234 in the western Arctic Ocean, *Acta Oceanol. Sin.*, 24(6), 97–108.
- Mackey, M., D. Mackey, H. Higgins, and S. Wright (1996), CHEMTAX—A program for estimating class abundances from chemical markers: Application to HPLC measurements of phytoplankton, *Mar. Ecol. Ser.*, 144, 265–283.
- Mackinson, B. L., S. B. Moran, M. W. Lomas, G. M. Stewart, and R. P. Kelly (2015), Estimates of micro-, nano-, and picoplankton contributions to particle export in the northeast Pacific, *Biogeosciences*, 12(11), 3429–3446, doi:10.5194/bg-12-3429-2015.
- Masqué, P., J. K. Cochran, D. J. Hirschberg, D. Dethleff, D. Hebbeln, A. Winkler, and S. Pfirman (2007), Radionuclides in Arctic sea ice: Tracers of sources, fates and ice transit time scales, *Deep-Sea Res., Part I*, 54(8), 1289–1310, doi:10.1016/j.dsr.2007.04.016.
- Matrai, P. A., E. Olson, S. Suttles, V. Hill, L. A. Codispoti, B. Light, and M. Steele (2013), Synthesis of primary production in the Arctic Ocean: I. Surface waters, 1954–2007, *Prog. Oceanogr.*, 110, 93–106, doi:10.1016/j.pocean.2012.11.004.
- Melnikov, I. A., and L. L. Bondarchuk (1987), Ecology of mass accumulations of colonial diatom algae under drifting Arctic ice, *Oceanology*, 27(2), 233–236, doi:10.1594/PANGAEA.756627.
- Metfies, K., W.-J. von Appen, E. Kilias, A. Nicolaus, and E.-M. Nöthig (2016), Biogeography and photosynthetic biomass of arctic marine pico-eukaryotes during summer of the record sea ice minimum 2012, *PLoS One*, 11(2), e0148512, doi:10.1371/journal.pone.0148512.
- Moore, R. M., and J. N. Smith (1986), Disequilibrium between ²²⁶Ra, ²¹⁰Pb and ²¹⁰Po in the Arctic Ocean and the implications for chemical modification of the Pacific water inflow, *Earth Planet. Sci. Lett.*, 77(3–4), 285–292, doi:10.1016/0012-821X(86)90140-8.
- Moran, S. B., and J. N. Smith (2000), ²³⁴Th as a tracer of scavenging and particle export in the Beaufort Sea, *Cont. Shelf Res.*, 20(2), 153–167, doi:10.1016/S0278-4343(99)00065-5.
- Moran, S. B., K. M. Ellis, and J. N. Smith (1997), ²³⁴Th/²³⁸U disequilibrium in the central Arctic Ocean: Implications for particulate organic carbon export, *Deep-Sea Res., Part II*, 44(8), 1593–1606, doi:10.1016/S0967-0645(97)00049-0.
- Moran, S. B., et al. (2005), Seasonal changes in POC export flux in the Chukchi Sea and implications for water column–benthic coupling in Arctic shelves, *Deep-Sea Res., Part II*, 52(24–26), 3427–3451, doi:10.1016/j.dsr2.2005.09.011.

- Murray, J. W., B. Paul, J. P. Dunne, and T. Chapin (2005), ^{234}Th , ^{210}Pb , ^{210}Po and stable Pb in the central equatorial Pacific: Tracers for particle cycling, *Deep-Sea Res., Part I*, 52(11), 2109–2139, doi:10.1016/j.dsr.2005.06.016.
- Nicolaus, M., C. Katlein, J. Maslanik, and S. Hendricks (2012), Changes in Arctic sea ice result in increasing light transmittance and absorption, *Geophys. Res. Lett.*, 39, L24501, doi:10.1029/2012GL053738.
- Noji, T. T., U. V. Bathmann, B. von Bodungen, M. Voss, A. Antia, M. Krumbholz, B. Klein, I. Peeken, C. I.-M. Noji, and F. Rey (1997), Clearance of picoplankton-sized particles and formation of rapidly sinking aggregates by the pteropod, *Limacina retroversa*, *J. Plankton Res.*, 19, 863–875, doi:10.1093/plankt/19.7.863.
- Not, C., K. Brown, B. Ghaleb, and C. Hillaire-Marcel (2012), Conservative behavior of uranium vs. salinity in Arctic sea ice and brine, *Mar. Chem.*, 130–131, 33–39, doi:10.1016/j.marchem.2011.12.005.
- Olli, K., et al. (2007), The fate of production in the central Arctic Ocean—Top-down regulation by zooplankton expatriates?, *Prog. Oceanogr.*, 72(1), 84–113, doi:10.1016/j.pocean.2006.08.002.
- Overland, J. E., and M. Wang (2013), When will the summer Arctic be nearly sea ice free?, *Geophys. Res. Lett.*, 40, 2097–2101, doi:10.1002/grl.50316.
- Owens, S. A., K. O. Buesseler, and K. W. W. Sims (2011), Re-evaluating the ^{238}U -salinity relationship in seawater: Implications for the ^{238}U - ^{234}Th disequilibrium method, *Mar. Chem.*, 127(1–4), 31–39, doi:10.1016/j.marchem.2011.07.005.
- Parkinson, C. L., and J. C. Comiso (2013), On the 2012 record low Arctic sea ice cover: Combined impact of preconditioning and an August storm, *Geophys. Res. Lett.*, 40, 1356–1361, doi:10.1002/grl.50349.
- Passow, U. (2002), Transparent exopolymer particles (TEP) in aquatic environments, *Prog. Oceanogr.*, 55(3–4), 287–333, doi:10.1016/S0079-6611(02)00138-6.
- Pike, S., K. Buesseler, J. Andrews, and N. Savoye (2005), Quantification of ^{234}Th recovery in small volume sea water samples by inductively coupled plasma-mass spectrometry, *J. Radioanal. Nucl. Chem.*, 263(2), 355–360, doi:10.1007/s10967-005-0594-z.
- Puigcorbé, V., C. R. Benitez-Nelson, P. Masqué, E. Verdeny, A. E. White, B. N. Popp, F. G. Prahl, and P. J. Lam (2015), Small phytoplankton drive high summertime carbon and nutrient export in the Gulf of California and Eastern Tropical North Pacific, *Global Biogeochem. Cycles*, 29, 1309–1332, doi:10.1002/2015GB005134.
- Puigcorbé, V., et al. (2016), Particulate organic carbon export across the Antarctic Circumpolar Current at 10°E: Differences between north and south of the Antarctic Polar Front, *Deep-Sea Res., Part II*, doi:10.1016/j.dsr2.2016.05.016, in press.
- Quigley, M. S., P. H. Santschi, C.-C. Hung, L. Guo, and B. D. Honeyman (2002), Importance of acid polysaccharides for ^{234}Th complexation to marine organic matter, *Limnol. Oceanogr.*, 47(2), 367–377, doi:10.4319/lo.2002.47.2.0367.
- Richardson, T. L., and G. A. Jackson (2007), Small phytoplankton and carbon export from the surface ocean, *Science*, 315(5813), 838–840, doi:10.1126/science.1133471.
- Rigaud, S., V. Puigcorbé, P. Cámara-Mor, N. Casacuberta, M. Roca-Martí, J. Garcia-Orellana, C. R. Benitez-Nelson, P. Masqué, and T. Church (2013), A methods assessment and recommendations for improving calculations and reducing uncertainties in the determination of ^{210}Po and ^{210}Pb activities in seawater, *Limnol. Oceanogr. Methods*, 11(10), 561–571, doi:10.4319/lom.2013.11.561.
- Roberts, K. A., J. K. Cochran, and C. Barnes (1997), ^{210}Pb and $^{239,240}\text{Pu}$ in the Northeast Water Polynya, Greenland: Particle dynamics and sediment mixing rates, *J. Mar. Syst.*, 10(1–4), 401–413, doi:10.1016/S0924-7963(96)00061-9.
- Roca-Martí, M., V. Puigcorbé, M. H. Iversen, M. M. Rutgers van der Loeff, C. Klaas, W. Cheah, A. Bracher, and P. Masqué (2016), High particulate organic carbon export during the decline of a vast diatom bloom in the Atlantic sector of the Southern Ocean, *Deep-Sea Res., Part II*, doi:10.1016/j.dsr2.2015.12.007, in press.
- Rodriguez y Baena, A. M., S. W. Fowler, and J. C. Miquel (2007), Particulate organic carbon: Natural radionuclide ratios in zooplankton and their freshly produced fecal pellets from the NW Mediterranean (MedFlux 2005), *Limnol. Oceanogr.*, 52(3), 966–974, doi:10.4319/lo.2007.52.3.0966.
- Rudels, B. (2009), Arctic Ocean Circulation, in *Ocean Currents: A Derivative of the Encyclopedia of Ocean Sciences*, edited by J. H. Steele, S. A. Thorpe, and K. K. Turekian, pp. 211–225, Academic Press, London, U. K.
- Rutgers van der Loeff, M. M., et al. (2006), A review of present techniques and methodological advances in analyzing ^{234}Th in aquatic systems, *Mar. Chem.*, 100(3–4), 190–212, doi:10.1016/j.marchem.2005.10.012.
- Savoye, N., C. Benitez-Nelson, A. B. Burd, J. K. Cochran, M. Charette, K. O. Buesseler, G. A. Jackson, M. Roy-Barman, S. Schmidt, and M. Elskens (2006), ^{234}Th sorption and export models in the water column: A review, *Mar. Chem.*, 100(3–4), 234–249, doi:10.1016/j.marchem.2005.10.014.
- Shaw, W. J., T. P. Stanton, M. G. McPhee, J. H. Morison, and D. G. Martinson (2009), Role of the upper ocean in the energy budget of Arctic sea ice during SHEBA, *J. Geophys. Res.*, 114, C06012, doi:10.1029/2008JC004991.
- Sherr, E. B., B. F. Sherr, P. A. Wheeler, and K. Thompson (2003), Temporal and spatial variation in stocks of autotrophic and heterotrophic microbes in the upper water column of the central Arctic Ocean, *Deep-Sea Res., Part I*, 50(5), 557–571, doi:10.1016/S0967-0637(03)00031-1.
- Shimmield, G. B., G. D. Ritchie, and T. W. Fileman (1995), The impact of marginal ice zone processes on the distribution of ^{210}Pb , ^{210}Po and ^{234}Th and implications for new production in the Bellingshausen Sea, Antarctica, *Deep-Sea Res., Part II*, 42(4–5), 1313–1335, doi:10.1016/0967-0645(95)00071-W.
- Smith, J., S. Moran, and R. Macdonald (2003), Shelf-basin interactions in the Arctic Ocean based on ^{210}Pb and Ra isotope tracer distributions, *Deep-Sea Res., Part I*, 50(3), 397–416, doi:10.1016/S0967-0637(02)00166-8.
- Smith, J. N., and K. M. Ellis (1995), Radionuclide tracer profiles at the CESAR Ice Station and Canadian Ice Island in the western Arctic Ocean, *Deep-Sea Res., Part II*, 42(6), 1449–1470, doi:10.1016/0967-0645(95)00049-6.
- Smith, R. E. H., M. Gosselin, and S. Taguchi (1997), The influence of major inorganic nutrients on the growth and physiology of high arctic ice algae, *J. Mar. Syst.*, 11(1–2), 63–70, doi:10.1016/S0924-7963(96)00028-0.
- Spreen, G., L. Kaleschke, and G. Heygster (2008), Sea ice remote sensing using AMSR-E 89-GHz channels, *J. Geophys. Res.*, 113, C02S03, doi:10.1029/2005JC003384.
- Stemann Nielsen, E. (1952), The use of radio-active carbon (C14) for measuring organic production in the sea, *J. Cons. Int. Explor. Mer.*, 18(2), 117–140, doi:10.1093/icesjms/18.2.117.
- Stewart, G., S. Fowler, J. L. Teyssié, O. Cotret, J. K. Cochran, and N. S. Fisher (2005), Contrasting transfer of polonium-210 and lead-210 across three trophic levels in marine plankton, *Mar. Ecol. Prog. Ser.*, 290, 27–33.
- Stewart, G., J. K. Cochran, J. C. Miquel, P. Masqué, J. Szlosek, A. M. Rodriguez y Baena, S. W. Fowler, B. Gasser, and D. J. Hirschberg (2007a), Comparing POC export from ^{234}Th / ^{238}U and ^{210}Po / ^{210}Pb disequilibria with estimates from sediment traps in the northwest Mediterranean, *Deep-Sea Res., Part I*, 54(9), 1549–1570, doi:10.1016/j.dsr.2007.06.005.
- Stewart, G., J. Kirk Cochran, J. Xue, C. Lee, S. G. Wakeham, R. A. Armstrong, P. Masqué, and J. Carlos Miquel (2007b), Exploring the connection between ^{210}Po and organic matter in the northwestern Mediterranean, *Deep-Sea Res., Part I*, 54(3), 415–427, doi:10.1016/j.dsr.2006.12.006.

- Stewart, G., S. B. Moran, M. W. Lomas, and R. P. Kelly (2011), Direct comparison of ^{210}Po , ^{234}Th and POC particle-size distributions and export fluxes at the Bermuda Atlantic Time-series Study (BATS) site, *J. Environ. Radioact.*, *102*(5), 479–489, doi:10.1016/j.jenvrad.2010.09.011.
- Stewart, G. M., S. Bradley Moran, and M. W. Lomas (2010), Seasonal POC fluxes at BATS estimated from ^{210}Po deficits, *Deep-Sea Res., Part I*, *57*(1), 113–124, doi:10.1016/j.dsr.2009.09.007.
- Taylor, B. B., E. Torrecilla, A. Bernhardt, M. H. Taylor, I. Peeken, R. Röttgers, J. Piera, and A. Bracher (2011), Bio-optical provinces in the eastern Atlantic Ocean and their biogeographical relevance, *Biogeosci. Discuss.*, *8*, 7165–7219.
- Tremblay, J.-É., L. G. Anderson, P. Matrai, P. Coupel, S. Bélanger, C. Michel, and M. Reigstad (2015), Global and regional drivers of nutrient supply, primary production and CO_2 drawdown in the changing Arctic Ocean, *Prog. Oceanogr.*, *139*, 171–196, doi:10.1016/j.pocean.2015.08.009.
- Trimble, S. M., and M. Baskaran (2005), The role of suspended particulate matter in ^{234}Th scavenging and ^{234}Th -derived export fluxes of POC in the Canada Basin of the Arctic Ocean, *Mar. Chem.*, *96*(1–2), 1–19, doi:10.1016/j.marchem.2004.10.003.
- Uitz, J., H. Claustre, A. Morel, and S. B. Hooker (2006), Vertical distribution of phytoplankton communities in open ocean: An assessment based on surface chlorophyll, *J. Geophys. Res.*, *111*, C08005, doi:10.1029/2005JC003207.
- Verdeny, E., P. Masqué, K. Maiti, J. Garcia-Orellana, J. M. Bruach, C. Mahaffey, and C. R. Benitez-Nelson (2008), Particle export within cyclonic Hawaiian lee eddies derived from ^{210}Pb – ^{210}Po disequilibrium, *Deep-Sea Res., Part II*, *55*(10–13), 1461–1472, doi:10.1016/j.dsr2.2008.02.009.
- Verdeny, E., P. Masqué, J. Garcia-Orellana, C. Hanfland, J. Kirk Cochran, and G. M. Stewart (2009), POC export from ocean surface waters by means of $^{234}\text{Th}/^{238}\text{U}$ and $^{210}\text{Po}/^{210}\text{Pb}$ disequilibria: A review of the use of two radiotracer pairs, *Deep-Sea Res., Part II*, *56*(18), 1502–1518, doi:10.1016/j.dsr2.2008.12.018.
- Waite, A. M., K. A. Safi, J. A. Hall, and S. D. Nodder (2000), Mass sedimentation of picoplankton embedded in organic aggregates, *Limnol. Oceanogr.*, *45*(1), 87–97, doi:10.4319/lo.2000.45.1.0087.
- Wassmann, P. (2011), Arctic marine ecosystems in an era of rapid climate change, *Prog. Oceanogr.*, *90*(1–4), 1–17, doi:10.1016/j.pocean.2011.02.002.
- Wei, C.-L., S.-Y. Lin, D. D.-D. Sheu, W.-C. Chou, M.-C. Yi, P. H. Santschi, and L.-S. Wen (2011), Particle-reactive radionuclides (^{234}Th , ^{210}Pb , ^{210}Po) as tracers for the estimation of export production in the South China Sea, *Biogeosciences*, *8*(12), 3793–3808, doi:10.5194/bg-8-3793-2011.
- Wilson, S., and D. K. Steinberg (2010), Autotrophic picoplankton in mesozooplankton guts: evidence of aggregate feeding in the mesopelagic zone and export of small phytoplankton, *Mar. Ecol. Prog. Ser.*, *412*, 11–27, doi:10.3354/meps08648.
- Yu, W., L. Chen, J. Cheng, J. He, M. Yin, and Z. Zeng (2010), ^{234}Th -derived particulate organic carbon export flux in the western Arctic Ocean, *Chin. J. Oceanol. Limnol.*, *28*(6), 1146–1151, doi:10.1007/s00343-010-9933-1.
- Yu, W., J. He, Y. Li, W. Lin, and L. Chen (2012), Particulate organic carbon export fluxes and validation of steady state model of ^{234}Th export in the Chukchi Sea, *Deep-Sea Res., Part II*, *81–84*, 63–71, doi:10.1016/j.dsr2.2012.03.003.
- Zhang, F., J. He, L. Lin, and H. Jin (2015), Dominance of picophytoplankton in the newly open surface water of the central Arctic Ocean, *Polar Biol.*, *38*(7), 1081–1089, doi:10.1007/s00300-015-1662-7.